JOURNAL OF GEOPHYSICAL RESEARCH, VOL. 103, NO. D24, PAGES 31,593-31,612, DECEMBER 27, 1998

Carbon dioxide transfer over a Central Amazonian rain forest

Yadvinder Malhi,[1] Antonio D. Nobre,[2] John Grace,[1] Bart Kruijt,[1] Maria G. P. Pereira,[2] Alistair Culf,[3] and Steve Scott[1]

Abstract. Tropical rain forests are among the most important and least monitored of terrestrial ecosystems. In recent years, their influence on atmospheric concentrations of carbon dioxide and water vapor has become the subject of much speculation. Here we present results from a yearlong study of CO_2 fluxes at a tropical forest in central Amazonia, using the micrometeorological technique of eddy covariance. The diurnal cycle of CO_2 flux was consistent with previous short-term studies in tropical rain forests, implying that the Amazonian rain forest shows a fair degree of spatial uniformity in bulk ecophysiological characteristics. Typical peak daytime photosynthesis rates were 24-28 μmol CO_2 m^{-2} s^{-1}, and respiration rates were 6-8 μmol CO_2 m^{-2} s^{-1}. There was significant seasonality in peak photosynthesis over the year, which appeared strongly correlated with soil moisture content. On the other hand, there was no evidence of strong seasonality in soil respiration. Central Amazonia has only a short, 3-month dry season, not atypical of tropical rain forest, and it is therefore likely that large areas of Amazonia exhibit significant seasonality in photosynthetic capacity. The gross primary production was calculated to be 30 t C ha^{-1} yr^{-1}. An analysis of data quality is included in the appendix.

1. Introduction

Considered globally, the most important interactions between the biosphere and the atmosphere are the transfers of energy, water, and carbon. Carbon is assimilated by the biosphere through photosynthesis and released through autotrophic (plant) and heterotrophic (animals, microbes, etc.) respiration. The magnitudes of these processes vary from biome to biome, but some of the largest fluxes are expected to be in tropical rain forests. These forests cover 12% of the planet's land surface and are estimated to contain 40% of the carbon in the terrestrial biosphere [*Whittaker and Likens*, 1975; *Taylor and Lloyd*, 1992]. They are responsible for approximately half of terrestrial gross primary productivity (that is, 8% of total atmospheric carbon dioxide is cycled through tropical rain forests every year [*Grace et al.*, 1998]). However, the gas-exchange properties of these forests have been much less studied than those of temperate and boreal forests.

Until recently, most investigations of forest CO_2 exchange relied on models to extrapolate short-term chamber measurements of gas exchange [e.g., *Farquhar et al.*, 1980; *Jarvis and Leverenz*, 1983]. This approach provides detailed understanding of processes at leaf and soil level but presents difficulties when attempting to scale up to whole ecosystems. In recent years, an alternative and complimentary approach has become available through the use of the eddy covariance technique to take long-term measurements of above-canopy CO_2 fluxes over a large patch of forest [*Baldocchi et al.*, 1996]. When combined with measurements of within-canopy storage of CO_2, these allow calculation of the total CO_2 exchange between the local biosphere and atmosphere.

The first eddy covariance study in tropical rain forests was by *Fan et al.* [1990] at the Ducke reserve near Manaus, Brazil (a site with vegetation and soil characteristics very similar to those described here). This was a pioneering but short-term study and was hampered by its functioning only in fair-weather conditions. More recently, *Grace et al.* [1995a, 1996] collected 50 days of almost continuous data in Reserva Jaru, Rondonia, Brazil (10°04.84'S, 61°56.60'W). This site is located toward the southern fringe of Amazonia, a region influenced by longer dry seasons and having more open, lower biomass forest (leaf area index 4.0, aboveground dry biomass 220 t ha^{-1}) and sandy soils. These data provided useful information on forest response to light and temperature and evidence that the forest was a net sink of carbon. However, there was still uncertainty as to the representativeness of the study site [*Keller et al.*, 1996] and to possible seasonal and interannual variations in the ecosystem carbon balance. In order to address this uncertainty, a new and ongoing eddy covariance study has been undertaken since 1995 at a second site near Manaus. This paper describes results from the first year of measurements at this site.

The primary focus of this paper is to examine and describe the nature and magnitude of the diurnal, seasonal, and annual CO_2 fluxes and their relationship to meteorological conditions and to discuss possible mechanisms for these variations. An empirical environmental response model is fitted to the data and then used to interpolate gaps to arrive at annual estimates of gross primary production and net ecosystem exchange. A more mechanistic exploration of the physiological constraints on photosynthesis and transpiration at this site is presented by *Williams et al.* [1998]. The water and energy budgets of this site and the issues surrounding the net carbon balance are discussed by (Y. Malhi et al., manuscript in preparation, 1998).

[1] Institute of Ecology and Resource Management, University of Edinburgh, Edinburgh, Scotland, United Kingdom.
[2] Instituto Nacional de Pesquisas da Amazonia, Manaus, Brazil.
[3] Institute of Hydrology, Wallingford, England, United Kingdom.

Paper number 98JD02647.
0148-0227/98/98JD-02647$09.00

2. Methods

2.1. Site

The measurements were made in the Reserva Biológica do Cuieiras (2°35'22"S, 60°06'55"W), a forest reserve belonging to the Instituto Nacional de Pesquisas da Amazônia (INPA), some 60 km north of Manaus, Amazonas, Brazil (see Figure. 1). This is part of a very extensive, continuous area of dense lowland terra firme tropical rain forest (mean annual rainfall, 2200 mm; canopy height, 30 m; aboveground dry biomass, 300-350 t ha^{-1}; leaf area index, 5-6). The area is inaccessible by river, was only made accessible by road in the 1970s, and is therefore not believed to have suffered past human disturbance. The soil on the plateau is a yellow clay latosol (Brazilian classification) or oxisol (U.S. Department of Agriculture soil taxonomy), with a high (80%) clay content, low nutrient content, low PH (4.3), and very high porosity (50-80% [*Chauvel et al.*, 1991]). However, much of the porosity is concentrated in the macropores and large mesopores, which drain rapidly, and in very fine pores containing water that is inaccessible to plants. This means that the available water capacity is low, only about 70 mm m^{-1} in the upper metre of the profile [*Correa*, 1984]. Further details on the hydraulic properties of this soil type are given by *Hodnett et al.* [1995]. This nutrient-poor soil type is typical of much of lowland Amazonia [*Sanchez*, 1989].

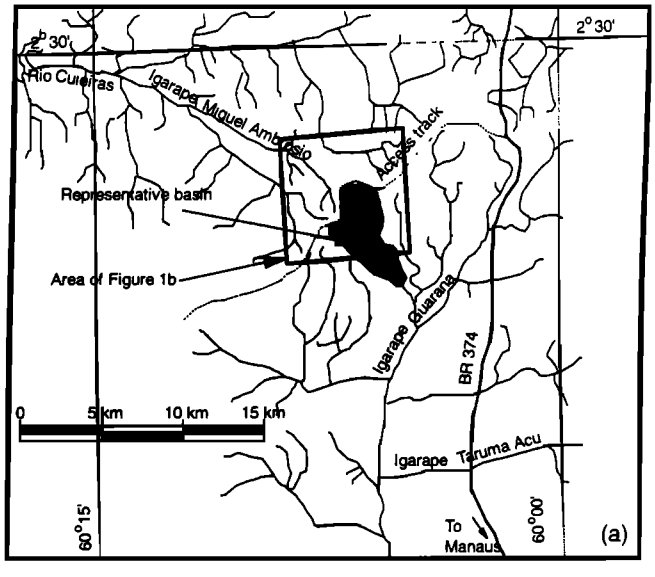

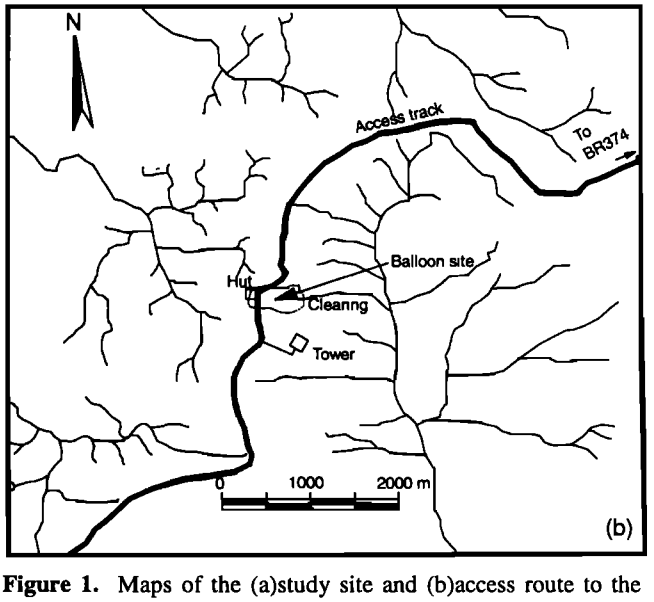

Figure 1. Maps of the (a)study site and (b)access route to the tower.

The study area is 40 km north of the Ducke reserve that was studied by *Fan et al.* [1990], but contains very similar forest. The Ducke forest may have a slightly more riverine climate and, more recently, may be influenced by the rapid urban expansion of Manaus. The climate of central Amazonia is characterized by high temperature, humidity, and rainfall. There is little variability in temperature (Manaus maximum daily temperature varies between 31°C and 33°C, and minimum daily temperature varies between 23°C and 24°C) but significant variation in rainfall (mean August rainfall, 50 mm; mean March rainfall, 330 mm), linked to the movement of the Intertropical Convergence Zone (ITCZ). The drier season typically lasts from mid-June to mid-October but can be very variable in length and intensity [*Hodnett et al.*, 1996].

The flux measurement station, an Edisol eddy covariance system [*Moncrieff et al.*, 1997], was mounted on a 41.5 m, 6.0 m cross-section tower, situated on an extensive plateau (90 m above sea level) dissected by occasional broad river valleys. The nearest human-disturbed region is the BR-174 road approximately 9 km to the east. The sensors were mounted 5 m above the tower (i.e., at a total height of 46.5 m) on its east pointing corner, so as to minimize flow distortion by the tower when the wind was blowing from its prevailing easterly direction (see below). The tower is larger than those usually used for eddy covariance work, and analyses of possible flow-distortion effects are presented in the appendix and by (Y. Malhi et al., manuscript in preparation, 1998). Access to the tower was by a track leading to an access road 1 km to the west.

2.2. Wind Direction and Fetch

The sampling area ("fetch") monitored by the eddy covariance system is determined by wind direction and, to a lesser extent, by the wind speed and thermal stratification of the atmospheric surface layer. Figure 2 shows the frequency distribution of wind direction over the study period, September 1, 1995, to August 31, 1996 (the wind direction readings may have a systematic error of up to 10°).

In sunny, daytime conditions (Figure 2a), the winds are overwhelmingly easterly, with the hourly averaged wind direction at high insolation (>500 W m^{-2}) lying between 0° and 180° for 84% of the time. This is due to the daytime convective boundary layer acquiring momentum from midtropospheric mean flow, which is linked to the general atmospheric circulation of trade winds at these latitudes. Thus the most common daytime wind direction oscillates between northeasterly (10°-60°) in November/December and southeasterly (90°-130°) in May/June, reflecting the differing influence of the northeasterly and southeasterly trades between the June and December solstices. All instances of daytime westerly winds are associated with local circulation around storm systems.

At night (Figure 2b) the boundary layer is decoupled from the mean tropospheric flow and there is a more uniform spread of wind directions. There is still some anisotropy, with a higher frequency of southeasterlies (30%) and a particularly low-frequency of southwesterlies (15%). The cause of this directional

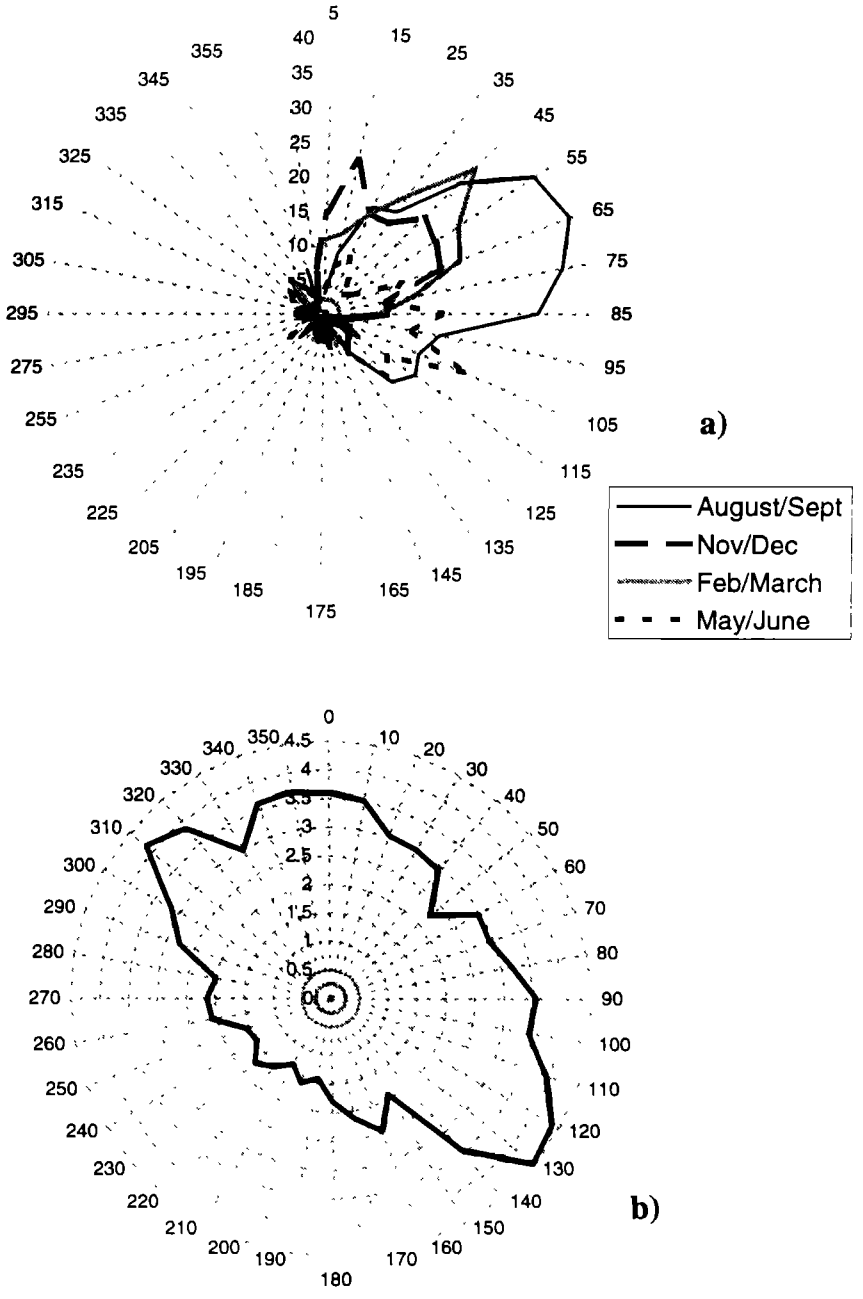

Figure 2. Wind direction distribution over the period September 1995 to August 1996; showing (a) daytime at high solar radiation (> 500 W m^{-2}) at various times of the year and (b) nighttime (1800-0500 LT). The scale on the radial axis is the percentage of the total data in each 10° bin.

bias is uncertain but may be linked to local topography and river-breeze effects.

Relative to the flux station, the body of the tower lies between 220° and 310° although flow edge effects may stretch slightly outside this band. Thus only 11% of the daytime and 18% of the nighttime winds come from this direction. An analysis of the possible effects of the tower on measured fluxes is presented in the appendix.

An estimate of the sampling area (fetch) of the flux system was made using a two-dimensional analytic solution of the diffusion equation proposed by *Schuepp et al.* [1990], together with a stability dependency proposed by *Lloyd* [1993]. In near-noon conditions, the Monin-Obukhov stability, $(z\text{-}d)/L$, typically varied between -1.5 and -0.2 (lower and upper quartiles, median = -0.6), and wind speed usually varied between 1.4 and 2.5 m s^{-1} (lower and upper quartiles, median = 1.9 m s^{-1}, mean = 2.0 m s^{-1}). Applying the *Schuepp et al.* [1990] model, we estimate that the central 50% of the measured flux originated between 40 and 290 m from the tower (peak at 100 m) and 90% of the flux originated between 20 and 1840 m. By multiplying the wind direction distribution (see above) with the fetch distribution, we estimate that the 50% flux footprint (i.e., the area from which the central 50% of the measured flux derives) covers an area of 18 ha (1 ha = 10^4 m) and the 90% footprint covers 255 ha. Applying a similar analysis to nighttime conditions (median stability, +1.5; quartile range, +0.4 to +4.2; median/mean wind speed, 1.4 m s^{-1}, quartile

range, 1.0 to 1.7 m s^{-1}), we estimate that the central 50% of the measured flux emanates from between 600 and 5600 m from the tower (peak at 1500 m) and 90% emanates from between 400 and 15,000 m from the tower. The 50% flux footprint covers an area of 4500 ha, and the 90% footprint covers 44,000 ha. Thus we calculate that the fetch area is much larger at night than during the day, partially owing to the more uniform wind direction distribution and partially owing to the longer turbulence dissipation time.

However, all these fetch estimates should be treated with caution and taken as only approximate indicators, as the planar source and surface layer similarity conditions for which the *Schuepp et al.* [1990] analysis is relevant are unlikely to be strictly applicable close to a forest canopy. Moreover, the intermittent nature of nocturnal turbulence is notoriously difficult to model, being characterized by intermittent local gust events rather than continual low-level turbulence. Thus it is probable that the nocturnal fetch is more local than that calculated here.

2.3. Instruments and Measurements

The technique of eddy covariance determines the CO_2 flux by calculating the covariance between fluctuations in vertical wind velocity and CO_2 concentration over all frequencies. Instantaneous vertical wind velocities were determined with a three-dimensional sonic anemometer (Solent, Gill Instruments, Lymington, England), and CO_2 concentrations were monitored by pumping the air sample at 6 dm^3 min^{-1} along 10 m of 6 mm teflon-lined Dekabon tubing to a fast response Li-6262 infrared gas analyzer (LICOR, Lincoln, Nebraska), sampled at an effective frequency of 5 Hz. The analogue output signal from the gas analyzer was sent to the sonic anemometer, where it was digitized and combined with the wind data. The combined digital output was collected at 20.8 Hz on a laptop computer, and fluxes were calculated in real time using University of Edinburgh Edisol software [*Moncrieff et al.*, 1997].

Vertical profiles of CO_2 and water vapor concentrations were monitored at six heights (1.0, 9.0, 17.4, 25.3, 33.3, and 46.5 m), with the topmost sample being the outflow from the eddy covariance system to permit consistency checks between the two instruments. The profile system sampled each height for 5 min, cycling through the entire profile every half hour. At each height, sufficient time was allowed to flush the tubing of residual air before sampling with an infrared gas analyzer (PP Systems, Hitchin, England). Vertical profiles of air temperature were monitored using thermocouples at six heights.

All instrumentation was powered using 10 Solarex MSX60 solar panels. The gas analyzers were calibrated at least weekly, using zero and fixed concentration CO_2 and water vapor samples (the fixed water vapor supply was generated using a Li-Cor Li-610 dew point generator). Very little drift in analyzer concentration was noted over a diurnal cycle or on a week-to-week basis, and even several parts per million drifts in measured CO_2 concentration have very little impact on flux measurements, which rely on monitoring fluctuations rather than absolute concentrations.

Meteorological data were collected with an automatic weather station operated by INPA, and soil moisture measurements were made manually by INPA staff using neutron probes at three access tubes in the vicinity of the tower, at approximately weekly frequency.

2.4. Data Continuity

The flux measurements were continuous in all weather, as the Solent anemometer is designed to function correctly in rainfall rates up to 300 mm h^{-1} (the effect of rain events on measured carbon fluxes is discussed in the appendix). However, large gaps in the data occurred because of instrument breakdown (probably because of near lightning strikes) and ensuing shipping and repair of instrumentation. Overall, 59% of the possible data between October 16, 1995 (the first measurement date), and August 15, 1996, were collected, and the gaps are not correlated to particular weather events. Over the full annual cycle discussed in this paper (September 1, 1995, to August 31, 1996), measured flux data are available for 54% of the time. The collected weather data were continuous throughout this annual cycle, with the only major malfunctions being occasional failure of the rain gauge.

The CO_2 and H_2O profile data were only collected for part of the experimental period, covering a period from October 20, to December 10, 1995.

2.5. Data Processing

The Edisol program detrended the concentrations and wind velocities (using a digital recursive filter, time constant 200 s, effective averaging period approximately 20 min) and rotated the wind field (u,v,w) coordinates such that mean v and w were zero over 10 min periods (for details, see *Moncrieff et al.* [1997]. Real-time data were collected as 10 min averages, but for several months, continuous raw data were also stored to evaluate the effect of the data processing routines on the calculated fluxes. The eddy timescale most responsible for scalar transport is approximately 20 s (~h/<u>; where instrument height, h = 46 m and mean wind speed, $\langle u \rangle \approx 2$ m s^{-1}); hence the 200 s time constant should be adequate.

Corrections were applied for the dampening of fluctuations at high frequencies using the approach outlined by *Moore* [1986] and *Moncrieff et al.* [1997]. Transfer functions were calculated for the loss of signal due to tube length, finite instrument response times, sensor separation and path length, and low-frequency signal loss due to detrending. These functions were applied to idealized surface layer covariance spectra (calculated from wind speed and stability using the semiempirical relations from *Kaimal et al.* [1972]), providing an estimate of the fractional loss of signal. The measured fluxes were then adjusted to allow for this loss term. A zero-plane displacement height of 20 m (2/3 of canopy height) was used. For CO_2 fluxes, the correction ranged from 10% to 25% in daytime conditions (mean =16%) and from 10% to 30% in nighttime conditions (mean=11%). An analysis of the measured spectra and their appropriateness for flux loss corrections is presented in the appendix.

Temperature fluctuations in the air samples were considerably damped by the 10 m length of the intake tube, but the final 2 m of the tube were made of copper to minimize fluctuations (an analysis by *Rannick et al.* [1997] suggests that a minimum length of 5 m is sufficient, and the use of copper tubing was not necessary). Therefore there was no need to apply the density fluctuation correction described by *Webb et al.* [1980].

Calculation of the within-canopy CO_2 storage required that the nonsynchronous measurements at different heights be interpolated in time to provide instantaneous profiles at half hour intervals and then that these profiles were interpolated vertically

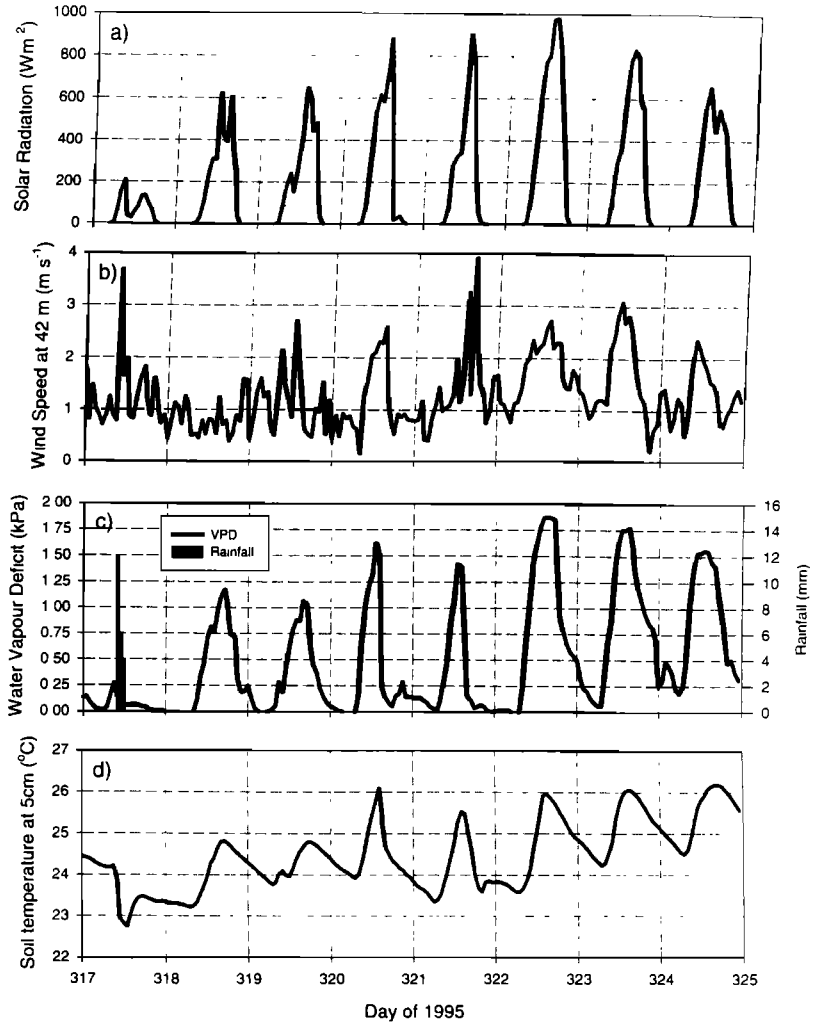

Figure 3. Hourly averaged meteorological data at 42 m height for a typical week (days 317 to 324, November 13 to 20, 1995), including (a) solar radiation, (b) wind speed, (c) water vapor deficit (VPD) and rainfall, and (d) soil temperature at 5 cm depth.

to estimate the total CO_2 stored. A cubic spline scheme was used for both interpolations.

3. Diurnal Patterns in CO_2 Fluxes

Figures 3 and 4 show the variation of hourly averaged solar radiation, rainfall, water vapor pressure deficit (VPD), wind speed, soil temperature at 5 cm depth, above-canopy CO_2 flux, within-canopy storage flux, and total biotic CO_2 flux over a typical week (days 317 to 324, November 13 to 20, 1995). Micrometeorological sign convention is followed for fluxes, with positive values indicating a flux away from the surface. This period demonstrates the contrast between overcast, rainy days (e.g., day 317, with maximum solar radiation 200 W m^{-2}, maximum daytime air temperature 23°C, maximum air VPD 0.2 kPa), and dry, sunny days (e.g., day 322, with maximum solar radiation, 970 W m^{-2}; maximum air temperature, 31°C; maximum air VPD, 1.85 kPa). There was a tendency for mist formation at night (indicated by VPD dropping to zero), particularly after rainy periods (e.g., night 318) and just before sunrise (e.g., nights 319 and 320). Soil temperature averaged about 24.5°C and exhibited a diurnal range of approximately 2°C, with maximum temperatures in the midafternoon and minimum temperatures at dawn. During a heavy rainfall event (e.g., day 317), the soil temperature would typically drop by 1-2°C, and these temperature drops are useful indicators of heavy rain events during periods when the rain gauge was not functioning.

Figure 5a shows the mean diurnal cycle of the above-canopy carbon flux, the within-canopy storage flux, and the biotic CO_2 flux or net ecosystem exchange (NEE) (derived as the sum of the other two fluxes) for the period October 16, 1995, to December 10, 1996. On average, the nocturnal respired CO_2 is equally partitioned between above-canopy flux (54%) and within-canopy storage (46%), though the situation on any particular night ranges from complete storage to complete emission, depending on meteorological conditions. As, on average, there is little evidence of a morning spike in above-canopy emissions, much of the nocturnally stored CO_2 is probably reabsorbed in morning photosynthesis.

The nature of the nocturnal CO_2 flux varies depending on

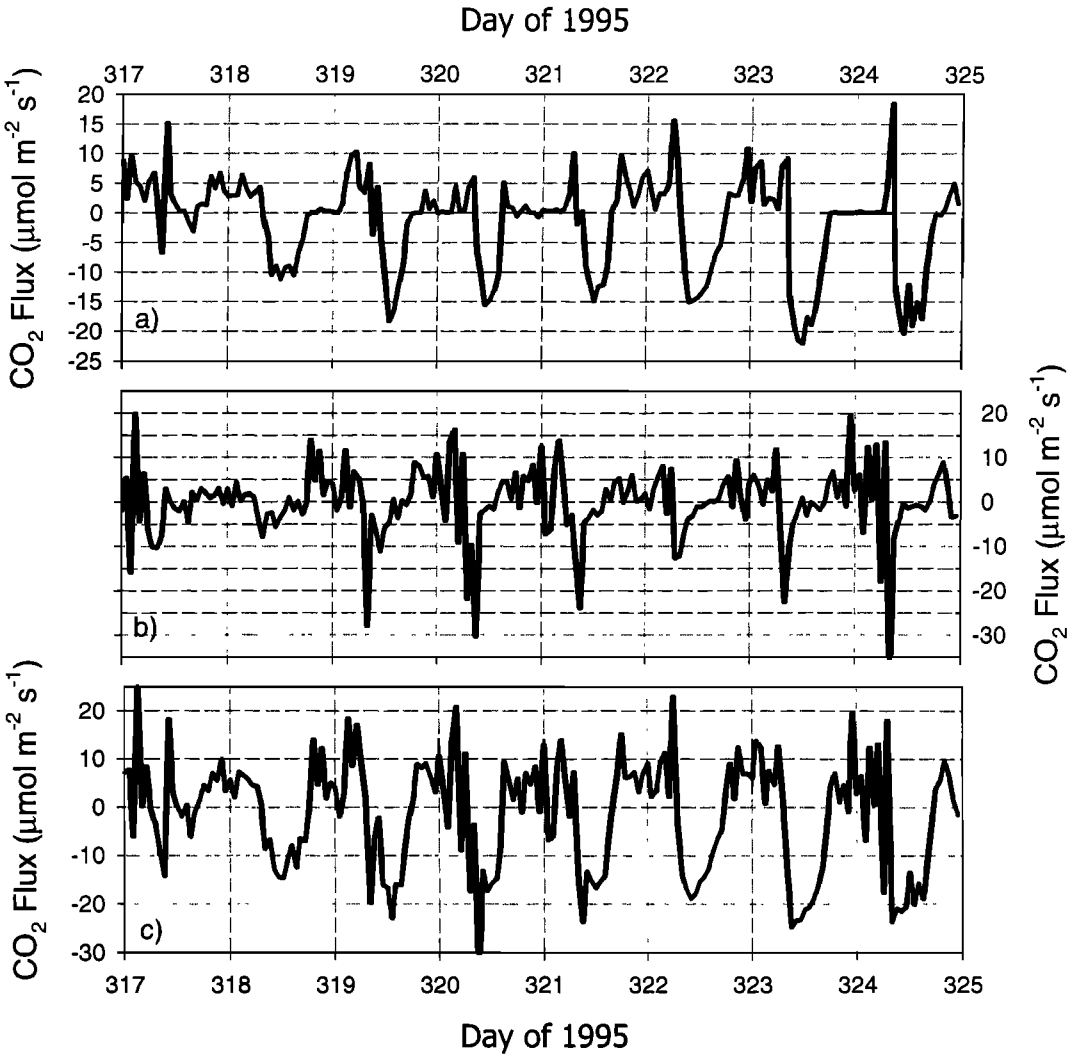

Figure 4. Hourly averaged CO_2 flux data for the same week as Figure 3, including (a) eddy covariance CO_2 flux at 46.5 m height, (b) flux of CO_2 into storage below 46.5 m (calculated from CO_2 profiles), and (c) total biotic CO_2 flux (or net ecosystem exchange (NEE)), derived as the sum of the other two fluxes.

meteorological conditions: on calm nights with very stable temperature stratification (e.g., 321 and 324), most of the respired CO_2 is stored within canopy, to be reabsorbed or released in a morning "flush," but on less stable nights (e.g., 318 and 322), most of the CO_2 is released intermittently throughout the night. The threshold friction velocity between these two states is approximately 0.1 m s^{-1} (see Figure A2). The atmospheric stability of any particular night is linked to wind speed and cloudiness and to the intensity of heating on the previous day. There is considerably more scatter in the storage flux data than in the above-canopy flux, because the within-canopy concentration measurements and the above-canopy flux measurements cover different sampling areas. If nocturnal CO_2 release is temporally and spatially intermittent, we would not expect the storage and above-canopy fluxes to be consistent on an hour-by-hour basis, but, as long as there is no systematic difference between the two sampling areas, we would expect the fluxes to be consistent as ensemble means. The latter appears to be largely true, but there is some evidence of undersampling by the profile system (see appendix).

The overall mean nocturnal NEE was 6.46±0.50 μmol CO_2 m^{-2} s^{-1} (95% confidence; number of samples, n=574; a description of possible systematic uncertainties with this estimate is provided in the appendix). The rate of photosynthesis increases rapidly after sunrise, with NEE reaching mean peak values of about -18 μmol m^{-2} s^{-1} between 0900 and 1100 LT, before beginning to decline. The standard error in the estimate of the hourly mean midday flux is 1.1 μmol m^{-2} s^{-1}, and that of the hourly nighttime flux is 0.8 μmol m^{-2} s^{-1}.

Figure 5b shows how the diurnal cycle of NEE varies between wet and dry seasons. As no within-canopy profiles were measured in the wet season, the mean storage flux cycle is assumed to be similar to that measured in October/November. The constancy of the derived nocturnal NEE shows that this is a reasonable assumption. In Figure 5b, "wet season" covers the period January 1 through March 31, 1996; "early dry" covers the period July 1 through August 15, 1996; and "late dry" is the period from October 16 to November 17, 1995. There is little variation in the nocturnal flux over the year, indicating little effect of varying soil temperature or soil moisture. The net

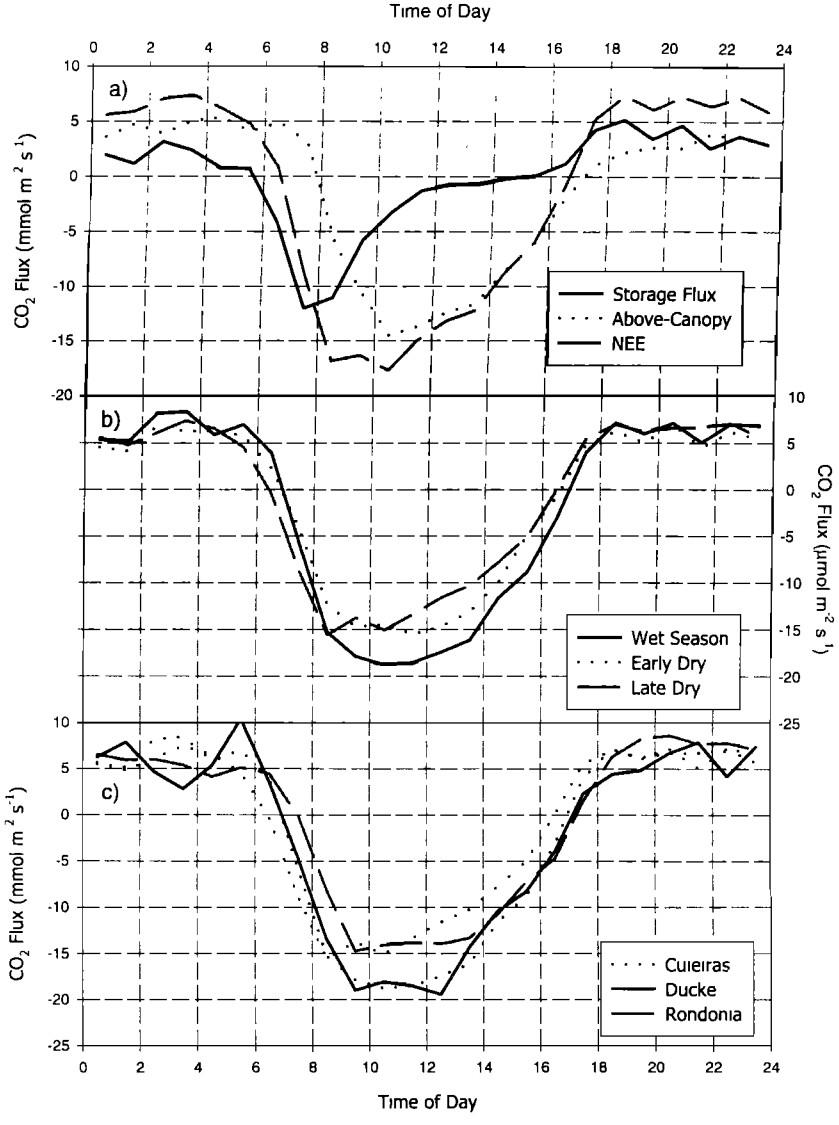

Figure 5. (a) Mean diurnal cycle of the above-canopy carbon flux, the within-canopy storage flux, and the net ecosystem exchange (NEE) for the period October 16 to December 10, 1995. (b) Variation of the diurnal cycle of NEE as it varies between wet and dry seasons, where "wet season" covers the period January 1 to March 31, 1996; "early dry" covers the period July 1 to August 15, 1996; and "late dry" is the period from October 16 to November 17, 1995. (c) Comparison of diurnal cycles of NEE at Reserva Cuieiras (this study), Reserva Ducke [*Fan et al.*, 1990], and Reserva Jaru (Rondonia) [*Grace et al.*, 1996].

daytime uptake, however, does show significant variation, peaking at –21 μmol m^{-2} s^{-1} in the wet season but only –17 μmol m^{-2} s^{-1} in the dry. In the wet and early dry seasons, the diurnal cycle is fairly symmetric about noon, peaking at about 1100 LT. In the late dry season, however, there is a significant afternoon cutback in photosynthesis, indicating the influence of soil moisture restrictions and high afternoon water vapor deficits (see section 6).

Figure 5c compares the diurnal cycle of NEE with those reported by *Fan et al.* [1990] for the nearby Ducke site in April/May 1987 (late wet season) and by *Grace et al.* [1996] for the site in Rondonia in southern Amazonia in April-June 1993 (late wet season). The daytime peak at the Ducke forest falls within the envelope between wet and dry season values at Cuieiras, and the lower biomass Rondonia forest shows a smaller peak value and greater asymmetry between morning and afternoon. There is no discernable difference in nighttime respiration, although the Ducke results have greater scatter owing to the smaller size of the data set. Taken together, these results suggest that, despite the high biodiversity, Amazonian terra firme rain forests show a remarkable spatial constancy in bulk ecophysiological function. In addition, the spatial variation across Amazonia (the difference between Cuieiras and Rondonia) seems to be of a similar magnitude to the seasonal variation at any one site (the difference between wet and dry seasons at Cuieiras).

4. Light-Response Curves

Figure 6a plots the hourly averaged biotic CO_2 flux against solar radiation for the period October 16 to December 10, 1995. All collected data with nonzero solar radiation are plotted.

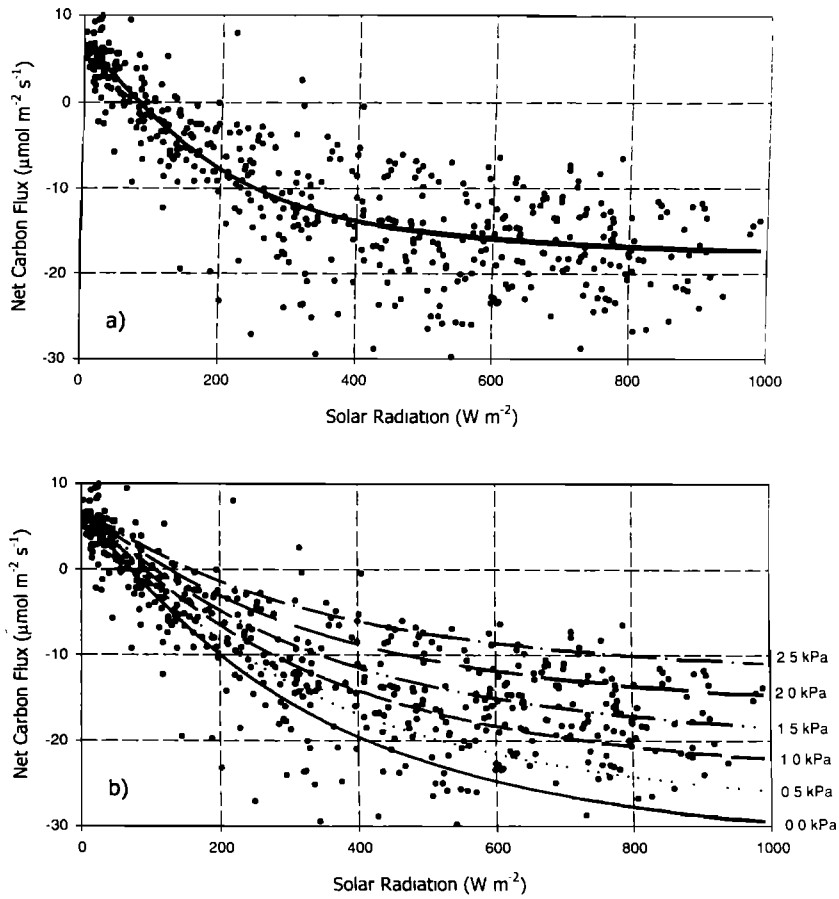

Figure 6. Hourly averaged biotic CO_2 flux against solar radiation for the period October 16 to December 10, 1995. The lines indicate the best fit with (a) no water vapor pressure deficit (VPD) response incorporated and (b) a linear VPD response (see text for equations).

The light response is linear at low incident solar radiation and appears to saturate at solar radiation >600 W m^{-2}. The ecosystem compensation point (when CO_2 release equals CO_2 uptake) occurs at insolations of 80±20 W m^{-2}, and the zero solar radiation intercept is +6.9 μmol CO_2 m^{-2} s^{-1}, close to the mean nighttime respiration of 6.5 calculated above.

The efficiency of forest photosynthesis can be assessed from the slope of the light-response curve. The theoretical maximum quantum yield for photosynthesis in leaves of C_3 species is about 0.06 mol CO_2 per mol absorbed photons (i.e., a quantum requirement of 17 absorbed photons per molecule of fixed CO_2 [*Farquhar et al.*, 1980]. At low light levels, when photosynthesis is limited by photon availability, the quantum yield should approach these maximum values, being restricted mainly by light absorption by nonphotosynthetic surfaces such as wood or soil. At higher insolations, however, other factors such as water availability and a finite maximum carboxylation rate may restrict the quantum yield.

If we assume that the photosynthetically active radiation flux (PAR) (μmol photons m^{-2} s^{-1}) = 2.16 × solar radiation [*Weiss and Norman*, 1985] and that absorbed PAR = 0.9 × incident PAR (the solar albedo of the site is approximately 12%), the overall apparent quantum efficiency of the forest (considering all data up to maximum insolation) in this period is 0.019 ± 0.0014 (95% confidence) mol CO_2 per mol absorbed photons (i.e., a quantum requirement of 52 ± 4 absorbed photons $molecule^{-1}$, 32% of theoretical maximum).

The maximum quantum yield can be assessed by considering the slope of the light-response curve at low solar radiation. Linear regression through all data less than 100 W m^{-2} gives an apparent quantum yield of 0.046±0.018 mol CO_2 per mol absorbed photons (i.e., 21 ± 10 absorbed photons $molecule^{-1}$, 77% of theoretical maximum). Fitting a nonrectangular hyperbolic equation to the entire data set (see section A5) suggests an apparent quantum yield of 0.045 (no VPD response) to 0.048 mol CO_2 per mol absorbed photons (including VPD response). The reflectivity of a forest canopy may decrease at low Sun angles, which would decrease the calculated quantum yield in low light conditions.

Table 1 compares the bulk ecophysiological properties of the Cuieiras study with those reported earlier for the Reserva Ducke forest [*Fan et al.*, 1990] and the Reserva Jarú [*Grace et al.*, 1995]. Despite a considerable range of structural and climatological variation, the bulk characteristics of all three Amazonian forests are remarkably similar. The central Ducke and Cuieiras forests (only 40 km apart) are particularly similar, whereas the more peripheral Jarú forest has lower quantum efficiency and photosynthetic rates, in accordance with its lower leaf area and biomass.

It appears that tropical forests can have a maximum photosynthetic efficiency very close to the theoretical maximum possible (as would be expected because of the high leaf area index), but other limiting factors can become important at even quite low solar radiation values. Taking all limiting factors into

Table 1. Comparison of Bulk Ecophysiological Properties in Three Eddy Covariance Studies in Tropical Rain Forests

Site Location	Duration of Study, Days	Aboveground Dry Biomass, t ha^{-1}	Leaf Area Index	Maximum Quantum Yield, mol CO_2 per mol absorbed photons	Dark Respiration, μmol CO_2 m^{-2} s^{-1}	Peak Photosynthesis, μmol CO_2 m^{-2} s^{-1}	Light Compensation Point, W m^{-2}	Overall Quantum Yield, μmol CO_2 m^{-2} s^{-1}	Estimated Annual Carbon Uptake, t C ha^{-1} yr^{-1}	Source
Ducke, near Manaus	12	300-350	5-6	0.051	6.0	27	120	0.17	2.2[c]	Fan *et al.* [1990]
Jarú, Rondonia	55	140-180	4	0.025	6.4	21	130	N/A	1.0[d]	Grace *et al.* [1995a]
Cuieiras, near Manaus	365	300-350	5-6	0.048	6.9	28[a], 16[b]	80	0.019	5.9	this study

[a] Wet season.
[b] Dry season.
[c] Extrapolated from mean measured uptake (8.1 t C ha^{-1} yr^{-1}) using solar radiation data.
[d] Extrapolated using fitted ecophysiological data. An alternative analysis of the data (Y. Malhi, unpublished data, 1998) suggests an uptake of 1.9 t C ha^{-1} yr^{-1}.

account, the overall photosynthetic efficiency of the Cuieiras and Ducke forests seems to be very similar, at 30% of the theoretical biochemical maximum.

An empirical environmental response model was fitted to the data. The aim of the model was to capture the mean behavior of the forest with as simple an equation as possible, allowing interpolation to fill in gaps in the data, rather than representing physiological processes in detail. The details of the model and fitting procedures are described in section A5.

The ecosystem respiration was modeled as an exponential function of the measured soil temperature, and photosynthesis was initially described purely as a nonrectangular hyperbolic function of incident solar radiation. The optimum fit had a coefficient of determination, r^2, of 0.68 and a convexity of 0.80. Introduction of a linear response to VPD improved the r^2 to 0.74 and reduced the convexity to 0.62, such that for a fixed VPD the photosynthesis did not saturate in high light conditions. In a review of eddy covariance studies, *Ruimy et al.* [1995] noted that all forests exhibit curvilinear light responses but not all fully saturate in high light conditions. In this (nonsaturating) case, the lower canopy may still be able to utilize extra light when upper canopy leaves are light saturated. Leaves in canopies at different levels saturate at different points along the light response curve, and therefore the canopy light response differs from individual leaf light response.

It must be emphasized that the model analysis does not conclude that there is a direct, process-based connection between VPD and photosynthesis but, rather, is only looking for a simple meteorological response model to allow gap interpolation. A more detailed analysis by *Williams et al.* [1998] suggests that soil moisture is the predominant constraint, and the relationship to VPD demonstrated above arises predominantly because of the correlation between soil moisture and VPD (compare Figures 7b and 9).

5. Seasonal Patterns

The climate in central Amazonia shows very little seasonal variation in temperature, or Sun angle but large changes in rainfall, with accompanying changes in soil and atmospheric water content. Figures 7 and 8 plot 24-hour values of total solar radiation, mean soil temperature, maximum water vapor pressure deficit, (monthly) rainfall, and mean albedo. All weather data except rainfall were continuous over the study period. There were several gaps in the rain data due to blockage of the rain gauge. In these periods, rain data from nearby sites at Fazenda Dimona (20 km to the north) and Reserva Ducke (40 km to the south) were used as substitutes; these substitute data appear reasonable at most periods, but the unusually low rainfall recorded in December and January (when Ducke data were used) may be the result of systematic differences between Ducke and Cuieiras (for a discussion of local spatial variability in rainfall, see *Ribeiro and Adis* [1984]).

The peak solar radiation on clear days is highest at the equinoxes, indicating a small Sun-angle effect, but, in general, cloudiness is a much stronger determinant of insolation. Low-insolation days correlate with lower air temperature, and rainfall events cause distinct drops in soil temperature. A strong seasonality is apparent in rainfall, but there is little variation in absolute humidity over the year. However, reduced evaporation in the dry season does induce a higher sensible heat flux and, consequently, higher air temperatures and much higher peak VPDs.

This seasonality in rainfall has an impact on canopy physiology, as evidenced by changes in canopy albedo (Figure 8b) and in the peak magnitudes of the net CO_2 flux (Figure 9). The albedo measurements show that the forest canopy is darker in the wet season. Any individual tower-based albedo measurement is unreliable, as the sampling area is small and may be overly influenced by the seasonal phenology of an individual tree, but *Culf et al.* [1995] report a very similar pattern in albedo at three other tower sites across Amazonia. They found that the albedo variations were strongly correlated to soil water content and not to cloudiness.

The peak photosynthetic rates show a surprisingly strong seasonal variation, as demonstrated in Figure 9, which plots the 10-day means of all CO_2 flux data at high insolation (> 600 W m^{-2}). The peak fluxes were typically -10 μmol m^{-2} s^{-1} in October (the first month of measurements), then rose rapidly with the onset of the wet season to typical values of approximately -20

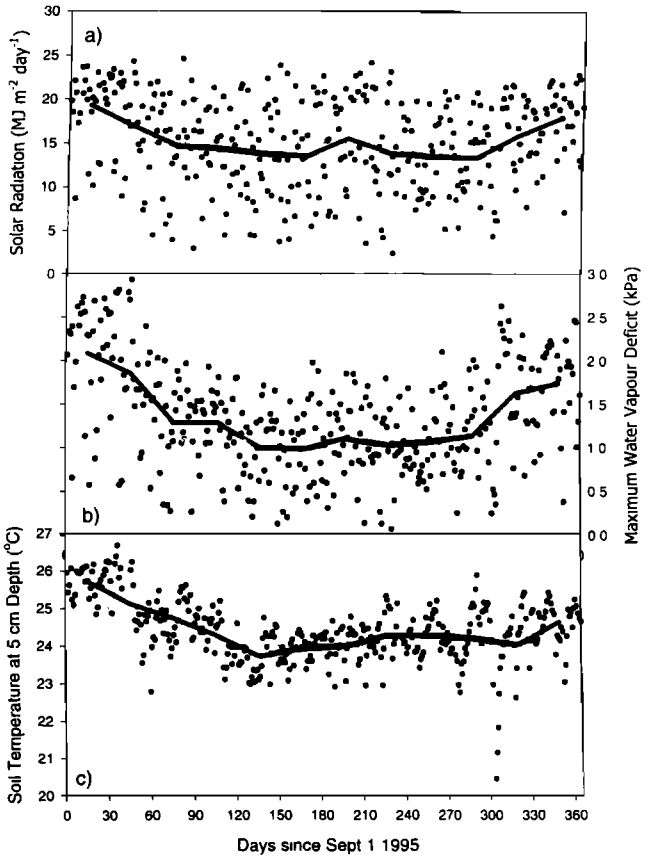

Figure 7. Twenty-four hour values of (a) total solar radiation, (b) maximum water vapor pressure deficit, and (c) mean soil temperature. The solid lines indicate monthly mean values.

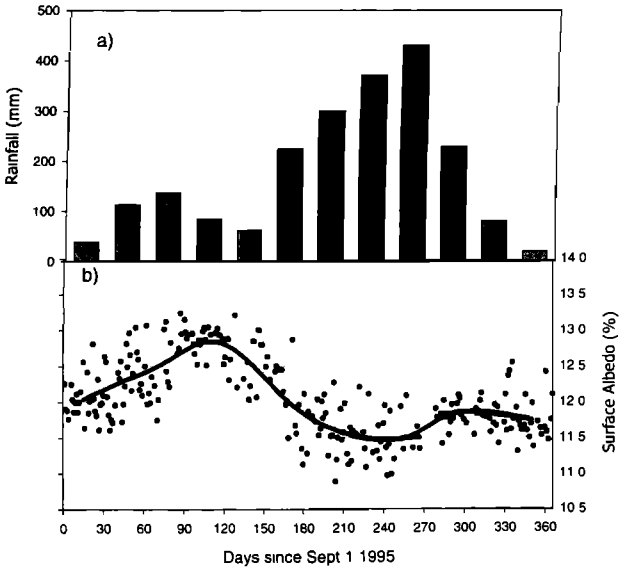

Figure 8. (a) Monthly rainfall and (b) mean albedo at 1100-1300 LT on sunny days (solar radiation > 500 W m^{-2}). The solid line indicates monthly mean albedo.

μmol m^{-2} s^{-1} in January, before slowly declining until August (the last month of measurements). The rise in photosynthetic capacity at the start of the wet season is particularly well correlated with changes in soil moisture (Figure 9); in the late wet season, photosynthetic capacity appears to decline more rapidly than soil moisture.

Figure 5b shows that there was little variation in the mean nocturnal fluxes and most of the seasonal variation is apparent only in high light conditions, indicating it is due to seasonal changes in photosynthesis rather than respiration. Some seasonality in respiration should be expected because of higher temperatures and greater moisture limitation in the dry season, but the present data cannot detect this. The small variation in mean soil temperature is unlikely to have a major effect; with a temperature sensitivity coefficient, Q_{10} = 2.3 [*Meir et al.*, 1996], (A1) suggests that soil temperature variation induces a change in monthly mean respiration between 6.7 μmol m^{-2} s^{-1} in the dry season and 5.7 μmol m^{-2} s^{-1} in the wet. Moisture limitation of microbial activity (decreasing respiration in the dry season) may be a more important seasonal factor, implying that the seasonality in photosynthesis must be even larger to generate the observed seasonality in net ecosystem exchange.

6. Discussion of Seasonality

The amplitude of the seasonal variation in peak photosynthesis is an unexpected phenomenon and is matched by a similar variation in transpiration. Further exploration of the links between rainfall, soil moisture, stomatal conductance, photosynthesis, and transpiration is performed in the work of *Williams et al.* [1998] and Y. Malhi et al., manuscript in preparation (1998), but an initial discussion is presented here.

The correlation with rainfall and soil moisture content (Figure 9) suggests that water stress is almost certainly the major environmental cause of the seasonality in photosynthesis. There are three (nonmutually exclusive) mechanisms that may explain how water stress impacts on bulk photosynthesis: (1) There is no change in biological characteristics such as leaf area or nutrient content, and the reduction in photosynthesis is simply a direct response of stomatal conductance to water stress, either in atmospheric demand or soil moisture supply. (2) There is a

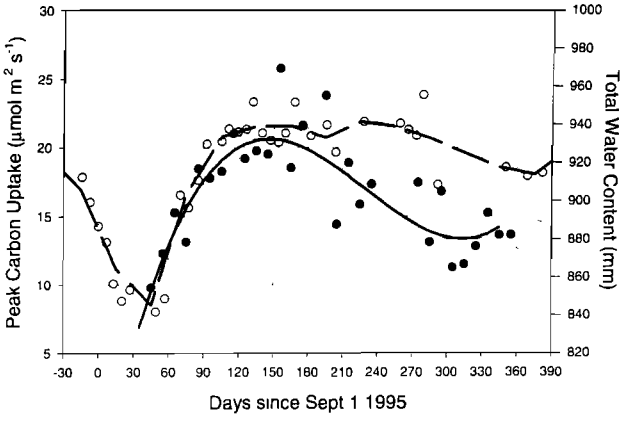

Figure 9. A comparison of peak daytime carbon uptakes rates, with total volumetric soil moisture content (0.0-2.0 m). Peak carbon uptake rates (solid circles) are calculated as 10 day means of above-canopy CO_2 fluxes at high insolation (> 600 W m^{-2}); the solid trend line is a third-order polynomial fit. Total volumetric water content (open circles) is from approximately weekly measurements; the dashed trend line is calculated from monthly averages.

phenological response in which leaf area and/or nutrient supply varies, which may be triggered directly by water stress or may be part of the general weakly deciduous character of the forest. (3) Water stress is having a direct impact on the biochemical mechanism of photosynthesis.

6.1. Direct Impacts of Water Stress

Although the absolute humidity does not vary significantly over the year, the higher dry season air temperature (caused by restricted transpiration and reduced cloudiness) does result in an increase in the VPD (Figure 7b). This, in turn, affects stomatal closure in the afternoon and hence net daytime photosynthesis.

A more important cause may be the drying of the soil during the dry season. The soil is a yellow clay latosol (90% clay), with a very high porosity but very low available water capacity. Figure 9 shows that the 0 to 2 m total volumetric water content decreasing from 940 mm (saturated soil) in the wet season to a minimum of 840 mm (all plant-extractable water removed) in the late dry season. The maximum water availability in the top 2 m is only 50 mm m^{-1}, and the remaining water is too tightly bound to the soil matrix to be extractable at biologically sustainable water potentials. The timing of the transition from dry to wet soil is strongly correlated with the measured increases in transpiration and photosynthesis, suggesting that soil moisture is indeed the key restricting factor. However, there is little evidence of restriction of soil water at deeper levels [*Hodnett et al.*, 1996] and much evidence that deep roots (up to 8 m) play an important role in maintaining dry season water supply in Amazonian forests [*Nepstad et al.*, 1994]. It may be that the water supply is sufficient to maintain the forest but that the increased hydraulic resistance (due to much reduced hydraulic conductivity in dry soil and reduced root area in contact with wet soil) is sufficient to require restrictions in transpiration and thus cause stomatal closure and a reduction in photosynthesis.

6.2. Indirect Impacts of Water Stress

An alternative to the direct soil moisture restriction hypothesis is the effect of phenological changes on photosynthesis. A number of studies [*Klinge et al.*, 1975; *Franken et al.*, 1979; *Luizão and Schubert*, 1989; *Luizão*, 1995] have reported strong seasonality in litter-fall rates in this region, with typical minimum litter-fall rates of 10-30 g m^{-2} $month^{-1}$ in January to February and maximum rates of 80-120 g m^{-2} $month^{-1}$ in the early dry season (June to August). Leaf shedding may be a direct response to drought conditions, but it may also represent a deliberate, partially deciduous strategy adopted by some tropical species to use the least advantageous part of the year as an opportunity to shed and renew photosynthetic tissue. In the latter case, it may be that the absolute dryness of any particular dry season has little impact on the amount of leaf shedding, but the timing of the onset of dryness is important as a trigger. On the other hand, onset of new growth may be triggered by photoperiod rather than rainfall [*Jordan*, 1983], a strategy which reduces the risk of new growth resulting from unusual heavy rain in the middle of the dry season.

Additional evidence is the asymmetry of the rapid increase in photosynthesis in the early wet season when compared to the slow decline in the later wet season and the fact that peak photosynthetic rates occur in January, 2 months before the peak of the wet season and 4 months before soil moisture content begins to decline. This suggests that the phenomenon causing the increase in photosynthesis is at least partially a response to the onset of rains, rather than being purely a response to soil water status. Corroborative evidence of seasonal variation in phenology is provided by the albedo measurements (Figure 8b).

Any individual tree or species of tree is likely to show a distinct amplitude and phase of seasonal change, and the net seasonal change observed reflects the mean of a multispecies consortium. In addition to changes in leaf area, other species-specific phenological factors (such as timing of flowering and fruiting) may have an impact on the seasonal pattern of net forest photosynthesis.

An additional possibility is that leaf nutrient content (in particular, nitrogen in the form of Rubisco) is reduced in the dry season. Drying of the upper soil restricts nutrient supply (through litter decay) and mobility within the soil and thus introduces nutrient restrictions to new growth. *Mello Ivo et al.* [1996] reported strong seasonal fluctuations in soil water concentrations of ammonium, calcium, sodium, magnesium, and potassium at a nearby site.

The relative influence of the various factors that may affect the seasonal cycle has been investigated by *Williams et al.* [1998] by application of a soil-plant atmosphere model. They concluded that leaf area changes have some impact but that, alone, were too small to explain the changes in photosynthesis. The litter-fall studies reported above suggest typical leaf area indices (LAI) of about 6 and a seasonal fluctuation in LAI of about 1. Most forest canopies approach high efficiency in light capture at values of LAI above 3, and a variation of LAI between 5 and 6 would not have much impact on either transpiration or photosynthesis. Similarly, application of an atmospheric VPD response accounted for only a small fraction of the seasonal variability. Only when a seasonal variation in soil hydraulic conductivity was introduced could the seasonal changes be accurately modeled. Thus changes in soil moisture availability and conductivity are the primary determinants of both photosynthesis and transpiration at this site; changes in atmospheric VPD and leaf area are secondary effects of these changes and have a small positive feedback on the amplitude and shape of the seasonal cycle.

6.3. Interannual Variability

The results and arguments presented herein suggest it is highly probable that water stress in the dry season has an impact on photosynthesis. However, it is important to place this dry season in the context of other years, which will only be possible at Cuieiras when additional years of rain data are collected. For example, 1995 was reported to be a drier-than-average year in central Amazonia, and it is possible that the impact of water stress may be less in other years. Figure 9 shows that the dry season in late 1996 was much weaker than that in 1995; volumetric soil moisture content (0.0-2.0 m) only dropped by 30 mm, compared with 100 mm in 1995. Conversely, 1997 had one of the most severe dry seasons on record in central Amazonia (associated with a strong El Niño event), and the forest appeared strongly water stressed. For the Ducke site, *Hodnett et al.* [1996] showed that the drying of the upper soil (and thus the requirement for deep extraction) varied enormously from year to year.

7. Ecosystem Characteristics

7.1. Net Ecosystem Exchange

A useful insight into the characteristics of the carbon balance of the ecosystem can be gained by considering the 24-hour totals of carbon fluxes and meteorological variables. Most of the

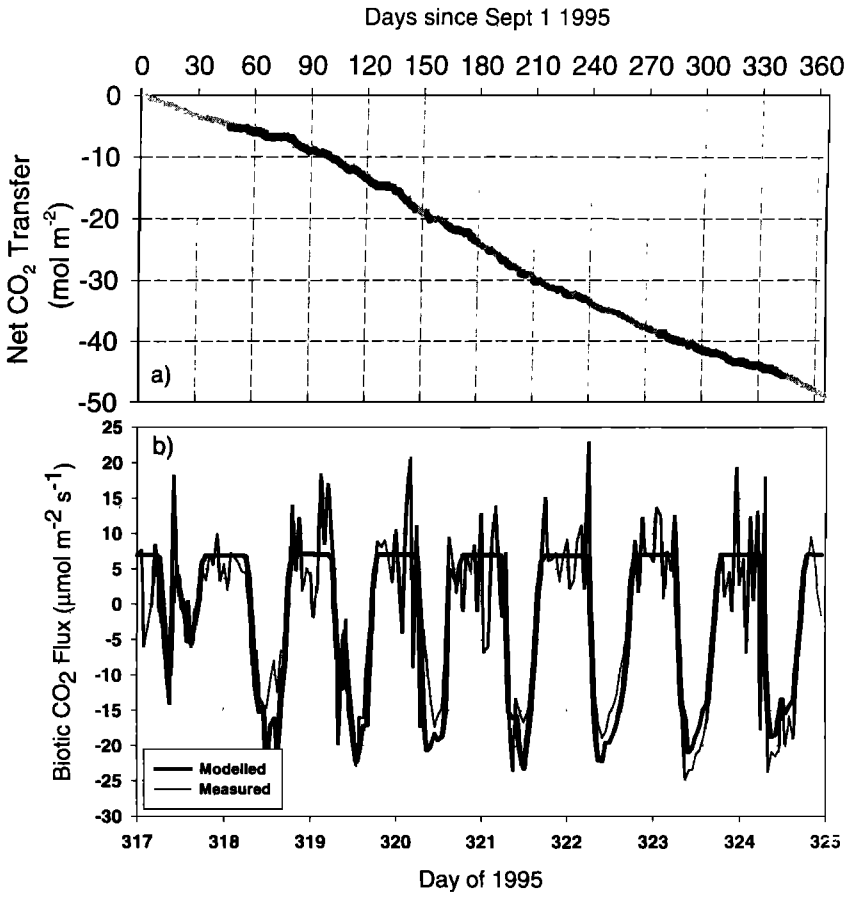

Figure 10. (a) Measured (solid line) and interpolated (stippled line) carbon accumulation over the year. (b) Match between measured (stippled line) and modeled biotic fluxes (solid line) over the week November 13 to 20, 1995 (days 317 to 324).

meteorological data were continuous over the year September 1, 1995, to August 31, 1996, but carbon flux data were only collected for 54% of the year. Hence it is necessary to use a meteorological response model to extrapolate carbon fluxes over the entire year. The details of the model are given in section A5. In addition to the response of respiration to soil temperature and the response of photosynthesis to light and VPD, the seasonality in peak photosynthesis was introduced as an additional variable. The maximum photosynthesis G_{max} was allowed to vary as a function of time of year and was found to be adequately decribed by a third-order polynomial: $G_{max} = (b_0 + b_1 d + b_2 d^2 + b_3 d^3)$ µmol m^{-2} s^{-1}, where b_0 = -25.05, b_1 = -0.18839, b_2 = 9.824×10^{-4}, b_3= -1.486×10^{-6}, and d = day since September 1, 1995).

Figure 10a shows the measured (solid line) and interpolated (stripped line) carbon accumulation over the year, and Figure 10b shows the match between measured and modeled biotic fluxes over the same week shown in Figures 3 and 4. The empirical fit to light and VPD captures most of the hourly variation of biotic flux but does not account for some of the day-to-day variability in peak photosynthetic rates. The noisiness in the nighttime flux on hourly timescales is due to the limited sampling area of the profile system, and the smooth efflux calculated by the model is probably closer to reality.

Over the year, the total estimated accumulation is 5.9 t C ha^{-1} yr^{-1}, a value that is considerably larger than the estimates of 1.0 t C ha^{-1} yr^{-1} for the site in Rondonia, and 2.2 t C ha^{-1} yr^{-1} for the Ducke forest (see Table 1). Although the basic diurnal cycle of CO_2 fluxes is very similar for all three sites (Figure 5c), only a small difference in bulk photosynthetic and respiratory fluxes can lead to large differences in net carbon balance. Thus, despite the similarity in bulk canopy physiology, we cannot conclude that all sites in Amazonia will demonstrate a similar net carbon uptake. The high uptake rates at the Cuieiras forest suggest that (1) there is a some error in the measured fluxes at Cuieiras that is not strongly apparent in the bulk fluxes but has an impact on the net flux, (2) the Cuieiras forest is showing a disproportionately large response to a global change signal, or (3) there is a more recent history of (probably natural) disturbance at Cuieiras. Possible mechanisms for natural disturbance include storm blowdowns, floods, drought, and forest fires. A recent study of biomass plots across Amazonia by *Phillips et al.* [1998] has demonstrated that there is considerable variability in the net carbon balance of forest plots according to local disturbance history, and the difference between the Rondonia, Ducke, and Cuieiras eddy covariance studies is entirely consistent with this variability. The contentious issue of net carbon balance is discussed in greater detail (Y. Malhi et al,. manuscript in preparation, 1998), where a comparison with local biomass studies is presented.

The pattern of the 24-hour net ecosystem exchange over the year is plotted in Figure 11a. Measured data points are shown as solid circles; model-derived points are open circles. The range of values is much larger in the wet season, when there is a greater spread of light conditions and greater sensitivity of photosynthesis to light, than in the dry season, when most days

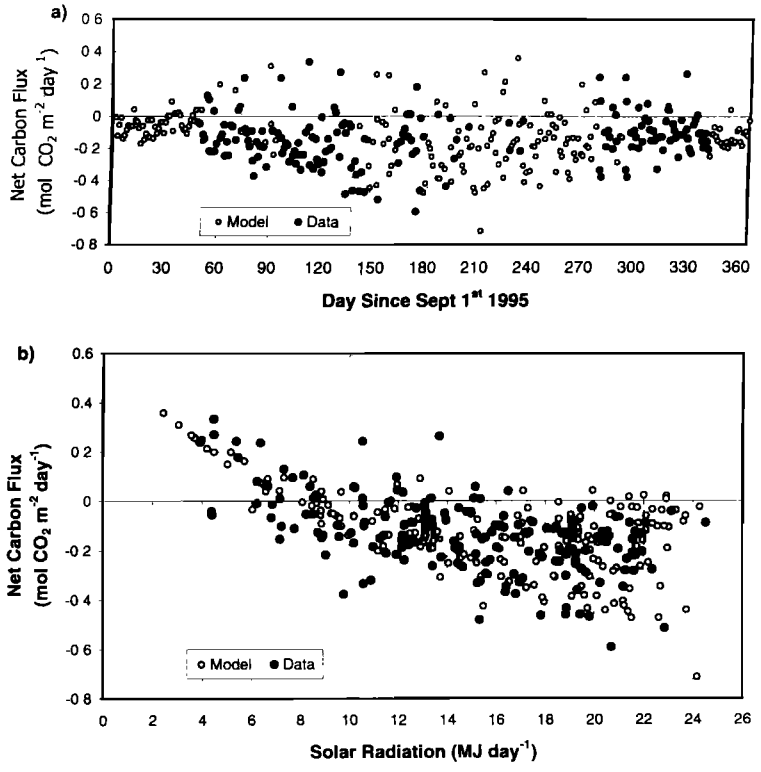

Figure 11. (a) The 24-hour net ecosystem exchange over the entire year. b) The 24-hour net ecosystem exchange against total daily insolation over the entire year.

are sunny and photosynthetic response inhibited. Thus the greatest CO_2 uptake and release rates are both found in the wet season. To some extent, the reduced photosynthetic capacity in the dry season is compensated for by the increased number of sunshine hours, and the amplitude of seasonal variation in actual photosynthesis is less than seasonal variation in photosynthetic capacity. However, the greater uptake rates are still found in the wet season.

Figure 11b plots the 24-hour net ecosystem exchange against total daily insolation over the entire year. The site is estimated to be a sink on 84% of days, with the threshold total daily insolation being 9 MJ. The range of values appears well constrained at low insolations but shows much greater spread at high insolation because of the seasonal variation in photosynthetic capacity.

7.2. Gross Primary Production

The gross primary production of the site (GPP = total carbon assimilation, incorporating photorespiration) can be estimated as follows (using micrometeorological sign convention): GPP = autotrophic respiration + heterotrophic respiration - NEE.

As a first approximation, the respiration can be assumed to be constant, and we take the mean-measured value of 6.46 μmol m^{-2} s^{-1}, corresponding to a total annual respiration of 24.5 t C yr^{-1}. Thus subtracting the total NEE calculated above (-5.91 t C ha^{-1} yr^{-1}) from the respiration, the total annual GPP is estimated to be 30.4 t C ha^{-1} yr^{-1}. Attaching a diurnal temperature response to the respiration makes little difference, as the mean nighttime and daytime soil temperatures are very similar; the total annual respiration and GPP are only increased by 0.4 t C ha^{-1} yr^{-1} each. If soil respiration is reduced in the dry season because of a moisture deficit, the September values of GPP may be higher than those indicated here.

This value of GPP is larger than the 24 t C ha^{-1} yr^{-1} estimated by *Lloyd et al.* [1995] for the lower biomass Rondonia forest. Previous estimates of GPP have been made from knowledge of net primary productivity and ecosystem respiration. In Côte d'Ivoire, *Müller and Nielsen* [1965] obtained a GPP of 25 t C ha^{-1} yr^{-1}, but at Pasoh forest in Malaysia, the corresponding figure was approximately double this value [*Oikawa*, 1985].

Using the value obtained for Cuieiras and multiplying by the area of tropical forest in the Amazon/Orinoco region (8.7 x 10^{12} m^2 [*Food and Agricultre Organization*, 1993), we estimate the GPP of Amazonian rain forest to be 26 Gt C yr^{-1} (about a quarter of the terrestrial production suggested by *Schimel* [1995]). This does not allow for the significant spatial heterogeneity, but it is difficult to assess this variability until a wider range of gas exchange and allometric studies are undertaken. The forests in the southern and eastern perimeter appear less productive, and it may be that the less water restricted forest on northwest Amazonia is more productive despite the higher cloudiness. The atmosphere contains approximately 765 Gt C as carbon dioxide; we therefore conclude that Amazonian rain forest processes 4% of the atmospheric CO_2 stock every year as gross production.

8. Conclusions

The data gathered at the Cuieiras forest allow, for the first time, an assessment of the variability of the bulk ecophysiological characteristics of a tropical rain forest on a seasonal timescale. In addition, comparison with the earlier data collected at Ducke and Rondonia enables us to draw tentative conclusions about the ecophysiology of the Amazonian terra firme rain forest as a whole.

It appears that factors such as spatial variability in species composition and soil type have, at most, only a secondary effect on bulk photosynthesis and respiration, and there is remarkable spatial consistency in the diurnal carbon cycle across Amazonia. This augurs well for modeling studies that attempt to scale up from single-site measurements to the Amazonian forest as a whole. The forest in Rondonia at the southern fringes of the rain forest does show lower peak photosynthesis, which is probably linked to the lower biomass and leaf area or, perhaps, more directly to the reduced water availability.

Although the bulk photosynthesis and respiration may show minor spatial variability, the net carbon balance is sensitive to small differences in these bulk fluxes and may show considerable spatial heterogeneity, depending on local site properties and natural disturbance history. This is evidenced by a recent synthesis of forest inventory data across Amazonia [*Phillips et al.*, 1998]. Thus using tower measurements to estimate the net carbon balance of Amazonian rain forest may yet prove a considerable challenge.

Whether directly or indirectly, it appears water availability can be a significant constraint on photosynthesis, even in tropical rain forest. The seasonality observed at the Cuieiras forest was unexpectedly large, though in hindsight, it does correlate well with evidence from canopy albedo and leaf litter fall. This seasonality would be expected to increase in strength toward the southern and eastern fringes of Amazonia, where the dry seasons are more severe, and diminish as one heads toward the perpetually wet northwest. It is possible that this may have some impact on the seasonal variation in global CO_2 concentration, analagous to that induced by northern forests, but the smaller magnitude of the tropical variation and the nonsynchronicity of dry seasons in various tropical forests would diminish this effect.

These speculations are, at the moment, rather tentative, and further research is needed, both on spatial variability and the effect of interannual variability in the length of the dry season. Moreover, attention needs to be focused on the mechanism of the water constraint. If, as predicted by some climate models, parts of Amazonia may be prone to increased dryness under the impact of global change, understanding the response of the forest to water stress may be crucial in predicting the carbon dynamics of the forest under possible future climate change.

Appendix: Checks on Data Quality and Gap Interpolation

A1. Spectral Analysis

The nature of the high-frequency correction applied is demonstrated in Figure A1, showing the cospectra of CO_2 concentration and vertical velocity, together with the semiempirical *Kaimal et al.*, [1972] cospectra and the corrected cospectra estimated from the transfer functions described above.

Cospectra were determined for 3 days and nights in December 1995 (December 5-7). All available 1 hour 20.8 Hz raw data were

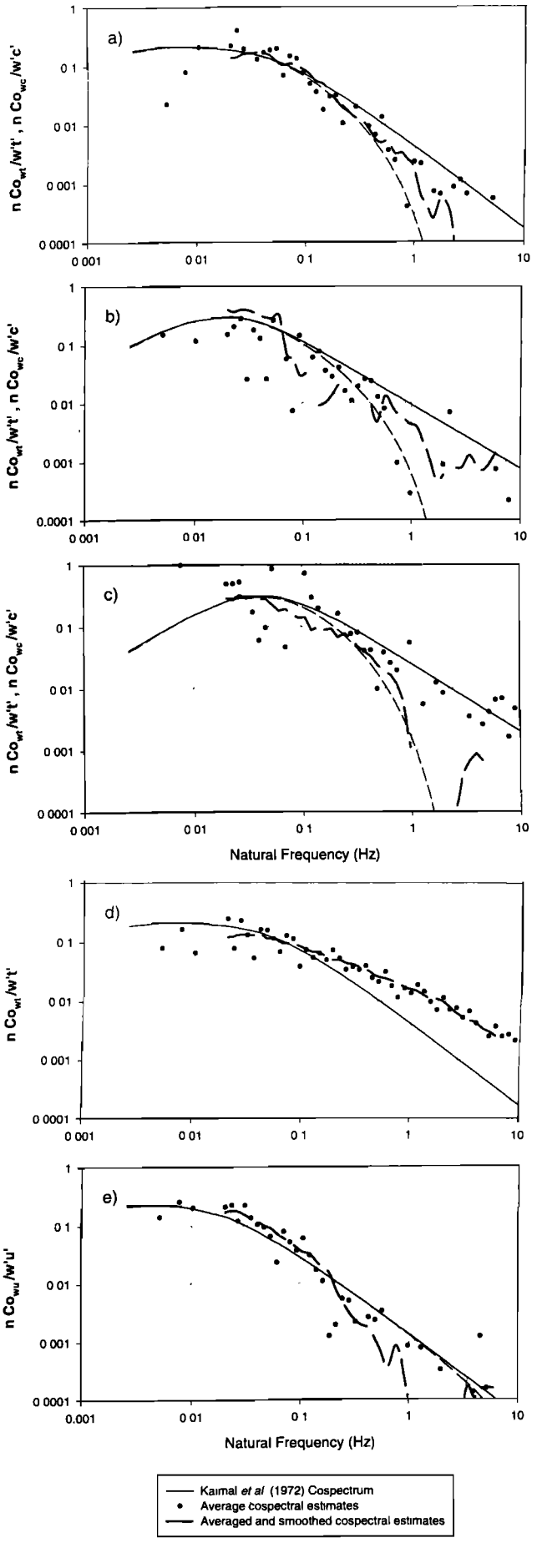

Figure A1. Cospectra of CO_2 concentration and vertical velocity, together with the semiempirical *Kaimal et al.* [1972] cospectra and the dampened cospectra estimated from transfer functions during (a) unstable conditions (daytime); (b) slightly stable conditions ($(z\text{-}d)/L < 0.26$), (c) highly stable conditions ($0.26<(z\text{-}d)/L < 2.6$). Measured and modelled cospectra in unstable conditions of (d) temperature and vertical velocity, and (e) horizontal and vertical velocity.

analyzed with Edispec software (J.M. Massheder, unpublished data, 1998). For each hourly data set, the program linearly detrended and performed a fast fourier transform (FFT) on nine 8192 point segments. No tapering or windowing was applied. Cospectra were averaged and log binned into 53 equally spaced log-frequency bins. The cospectra were then normalized by their integral over all frequencies and multiplied by their associated natural frequency.

Model spectra were calculated according to *Kaimal et al.* [1972], as modified by *Moore* [1986], as a function of measured atmospheric stability, wind speed, and estimated height over the zero plane (z-d = 26m). Low- and high-frequency transfer functions were then applied to the model spectra, accounting for flux underestimation resulting from filtering, sonic path averaging and separation, instrument response, damping in the tube, and response mismatch of sonic and gas analyzer [*Moore*, 1986; *Moncrieff et al.*, 1997].

The software was unable to evaluate spectral densities at low frequencies, making it hard to verify the location of the peak. Also, cospectra were normalized with their (relatively low) integral covariance, leading to higher normalized values than in the model. To facilitate comparison, the measured spectra were scaled by eye to match magnitude of the model spectra.

Figure A1a shows the averaged, normalized and scaled cospectra for the CO_2 flux in daytime conditions (an average of 29 hourly spectra), together with the model spectra for the sensible heat flux ($w't'$) and the predicted damped roll-off for the CO_2 flux cospectra. The turbulence is continuous, and there is excellent agreement between the predicted and observed damped *Kaimal et al.* [1972] cospectra, suggesting that (1) the surface-layer turbulence follows the Kaimal et al. relationships very closely and (2) the transfer function for fluctuation dampening by the instrumentation is being correctly estimated. In nighttime conditions, the shape of the cospectrum is dependent on surface-layer stability and shows much more variability. Indeed, the *Kaimal et al.* [1972] cospectra are of dubious applicability at even moderate stability, because of the increasingly intermittent nature of the turbulence. At low stabilities (Figure A1b; $(z\text{-}d)/L < 0.26$, average of 10 hourly cospectra) agreement to the predicted spectrum is still reasonable, but at higher stabilities (Figure A1c; $0.26<(z\text{-}d)/L < 2.6$, average of 18 hourly cospectra), there is much greater scatter but some evidence of a reduction of signal at high frequencies. This implies that more of the covariance signal is at low frequencies, where it is accurately measured by the instrumentation, and application of the high-frequency flux correction may lead to an overestimation of nighttime flux (but by usually less than 10%). However, the greater noisiness makes it difficult to calculate an alternative consistent flux correction. Fortunately, the absolute magnitude of the flux decreases with increasing stability, and thus the impact of this uncertainty diminishes even as its relative magnitude increases.

Figures A1d and A1e show measured and modeled spectra for $w't'$ and momentum flux ($w'u'$), respectively, for unstable cases only. These should be only slightly attenuated by damping and therefore serve as a test for the model spectra. The $w't'$ spectrum shows an unexpectedly shallow roll-off at high frequencies, with a slope close to -1 in the range 0.2 to 10 Hz. This suggests that the anisotropy of the turbulent production of $w't'$ still persists in the inertial cascade at these frequencies. Several studies have suggested that the spectrum at such production wavenumbers follows a -1 power law [e.g., *Katul et al.*, 1995]. The $w'u'$ cospectrum agrees well with the model except for at very high frequencies. Both spectra suggest a spectral peak at higher frequencies than predicted.

This apparent discrepancy between the spectral peak locations of model and measurements suggests that the instruments are located in the roughness sublayer, rather than in the surface layer. The spectral peak location is a function of the predominant turbulence length scale, which, in the *Kaimal et al.* [1972] model, is parameterized as (z-d) = 26 m. *Raupach et al.* [1996] have shown that within the "roughness sublayer" (between one and two canopy heights), turbulence length scales for vertical wind w are typically of order 0.3 h, where h is canopy height. Results of detailed canopy turbulence analysis, to be presented in a forthcoming paper, show that at the Cuieiras tower, integral length scales were even smaller than that. This would explain a spectral peak at apparently higher frequencies. Another explanation could be that vortices are shedding from some very tall trees in the surroundings, generating higher-frequency energy and short-circuiting the inertial subrange.

If the "real" inertial subrange is at higher frequencies, the flux loss corrections currently applied to the data would be underestimates of the true corrections required. However, the higher peaks in the spectra are not likely to imply a shift in the spectra as a whole but, rather, a broadening of the spectra. So, relative to the total covariance, the higher flux loss may be compensated by an increased flux at intermediate frequencies. We do not know of a spectral model to assess this quantitatively but would expect that such compensation limits the error in the relative flux corrections. Application of appropriate spectral models is a topic of ongoing research.

A2. Nighttime Respiration

A plot of the storage and aboveground components of the biotic flux against wind speed (Figure A2a) or the friction velocity u_* (Figure A2b) can be a useful test of the consistency of the profile and eddy flux measurements. At low wind speeds, the biotic flux is dominated by the storage component alone, whereas at high wind speeds, the above-canopy flux is more important. When plotted against wind speed, the biotic flux is reasonably constant, although there is evidence of a weak trend between 5.5 $\mu mol\ m^{-2}\ s^{-1}$ at 0.2 $m\ s^{-1}$ and 7.0 $\mu mol\ m^{-2}\ s^{-1}$ at 2.2 $m\ s^{-1}$. When plotted against u_*, however, the trend is more significant (P=1%; χ^2 test with null hypothesis of no trend, df=27). The variation is adequately described by a linear increase from 4.0 $\mu mol\ m^{-2}\ s^{-1}$ at 0.00 $m\ s^{-1}$ to 8.0 $\mu mol\ m^{-2}\ s^{-1}$ at 0.14 $m\ s^{-1}$ and a constant value of 8.0 $\mu mol\ m^{-2}\ s^{-1}$ at higher friction velocities.

The friction velocity would be expected to be more directly correlated to above-canopy flux than would the wind speed and may thus be a better discriminator of canopy-trapping and canopy-release conditions than is the wind speed. However, there is no reduction in scatter in the u_* plot compared with the wind speed plot. If genuine, the trend can have a number of possible explanations (ranked in a subjective order of likelihood):

1. The profile system is underestimating the nocturnal flux. This is possible if the small area sampled by the profile system is not representative of the wider area sampled by the flux system. It may also be that there is a substantial buildup of CO_2 very close (< 1 m) to the soil surface, which would not have been adequately sampled.

2. There is a net loss of flux from the system that is not measured by eddy covariance, and this loss is greater at low wind speeds. Examples may be lateral advection of respired CO_2, as

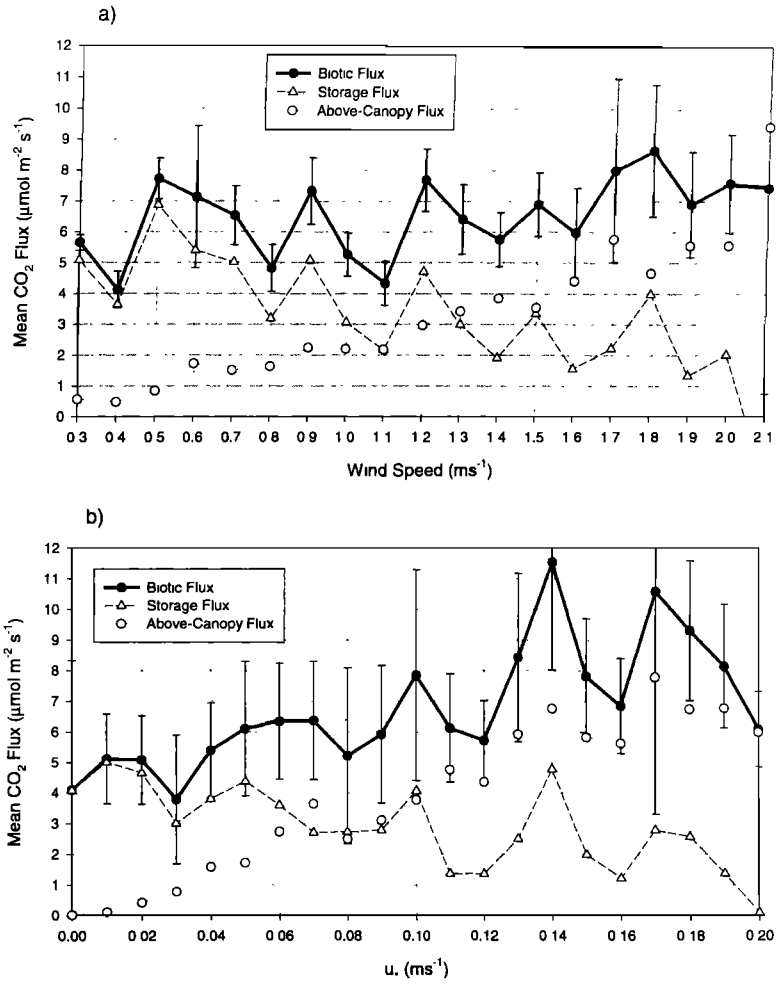

Figure A2. Storage and aboveground components of the biotic flux against (a) wind speed and (b) friction velocity u_*. The error bars shown are 95% confidence limits (assuming Gaussian distribution).

suggested by *Goulden et al.* [1996] for the Harvard forest study, or vertical transport at very low frequencies, which is not captured by the eddy covariance rotation and detrending schemes [*Lee*, 1998]. There is also still some uncertainty about the appropriateness of eddy covariance algorithms in nonstationary conditions.

3. There is a genuine response of respiration to u_*, for example, by increased release of CO_2 from soil pores in more turbulent conditions.

4. The eddy covariance system is somehow overestimating the daytime flux, although generally, flux measurements tend to miss a component of the flux, rather than add an artificial component.

Further insight into the reliability of the eddy covariance data can be gained by examining the 24-hour mean carbon uptake as measured by eddy covariance alone. As the magnitude of the storage term at 2400 Local Time (LT) will vary according to meteorological conditions, it is more reliable to calculate 24-hour aggregates of net carbon flux from 1700 LT of each day (rather than from 2400 LT), when the within-canopy storage is always close to zero. This 24-hour total is an independent measure of the net CO_2 exchange that does not rely on profile measurements. If factors accounting for variability in the daytime photosynthetic uptake can be eliminated, we can assess if the eddy covariance flux is sensitive to nighttime factors such as u_*. The two most important daytime factors to eliminate are the varying solar radiation and the seasonal variation in the peak photosynthetic uptake. The influence of varying solar radiation can be eliminated by only considering days when the total insolation is greater than 17 MJ, at which point the ecosystem light response flattens out (see Figure 11b). However, this still leaves considerable scatter in the data due to seasonal variation in photosynthetic capacity (Figure A3a) This seasonality can be factored out by normalizing the data with respect to the measured mean daytime CO_2 flux (here chosen as between 1100 and 1500 LT; early morning is avoided because of the possible biasing influence of stored CO_2). This normalization greatly reduces the scatter (Figure A3b), and the net CO_2 uptake is seen to be always negative and fairly constant, showing, at most, only a weak dependence on u_*, with NEE varying by about 0.6 µmol m^{-2} s^{-1} between u_* = 0.2 and 2.2 m s^{-1}.

Thus the trend of respired CO_2 with u_* is not apparent in the 24-hour mean eddy covariance data, suggesting that it is a problem with the profile measurements (i.e., explanation 1), rather than the eddy covariance. This, of course, has implications for our estimate of mean nocturnal respiration, suggesting that it may be as high as 8.0 µmol m^{-2} s^{-1} compared with our current estimate of 6.5 µmol m^{-2} s^{-1}. However, it is unwise to adjust for this factor until the exact nature of this phenomenon is better understood, and in the analysis presented in this paper, we retain the unadjusted measured values.

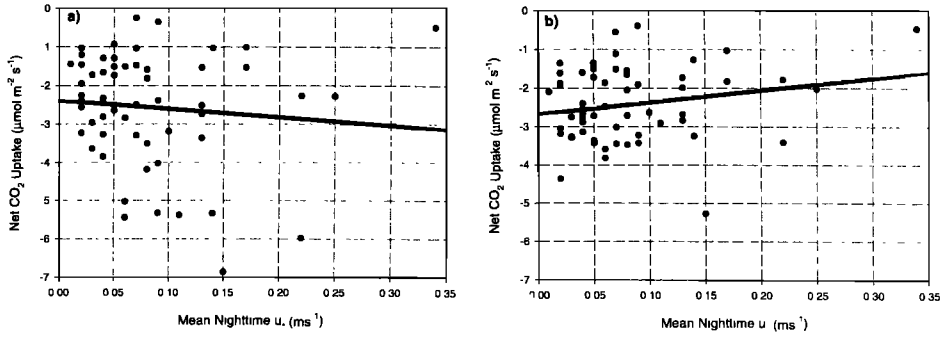

Figure A3. Twenty-four hour carbon uptake (considering only days with insolation > 17 MJ d^{-1}) against mean u_* of the previous night (over the time period 1800-0500 LT); (a) not normalized for varying daytime photosynthetic capacity and (b) normalized with respect to the mean CO_2 flux between 1100 and 1500 LT (see text).

A3. Variation of Measured Variables With Wind Direction

An analysis of the data with respect to wind direction enables evaluation of the spatial variability of the flux footprint area and possible disturbance effects due to the presence of the tower. An important factor to consider in this analysis is the very different distribution of wind directions at day and night (Figure 2).

A3.1. Nighttime Flux. Figure A4a shows how the nocturnal biotic flux varied with wind direction for the period October 16 to December 10, 1995. Nighttime is here defined as 1800 until 0500 LT, and all available data have been averaged into 45° bins. The 95% confidence limits are also plotted (assuming Gaussian distribution) and are approximately ±1.5 µmol CO_2 m^{-2} s^{-1}. Generally, the mean biotic flux varies between 5.0 and 7.2 µmol CO_2 m^{-2} s^{-1}, but there is a pronounced peak of 8.3 µmol CO_2 m^{-2} s^{-1} in the WNW segment (270°-315°). An analysis of variances shows that it is difficult to attach significance to the general pattern (analysis of variance (ANOVA) test; $df = 566$, $F = 2.127$, $P = 13\%$). However, a comparison of the WNW segment alone against the rest of the data suggests that the peak there is significant (Gaussian comparison, $P = 1.83\%$). This low significance is largely due to the noisiness of the data; a deviation from the mean would have to be greater than 3.3 µmol CO_2 m^{-2} s^{-1} to be significant at the 1% level.

The mean partitioning between within-canopy storage and above-canopy release shows weak variation with wind direction, with the above-canopy fraction being 45% in the southwest and 60% in the northeast. Interestingly, there is a proportional increase in both storage and above-canopy fluxes in the WNW segment, suggesting that the small spike in biotic flux in that direction is due to genuinely higher respiration, rather than flow distortion affecting the eddy covariance measurements.

A3.2. Daytime flux. The variation of daytime biotic flux with wind direction for the same period is shown in Figure A4b. Only the fluxes at high insolation (> 500 W m^{-2}) are plotted, to factor out correlation between cloudiness and wind direction. When winds are in the easterly segment, 345°-180°, the mean biotic flux varies between -16.8 and -18.3 µmol CO_2 m^{-2} s^{-1}, within the typical 95% confidence limits of ±1.5 µmol CO_2 m^{-2} s^{-1}. In the westerly segments, 180°-345°, the mean biotic flux is significantly smaller at -13.4 µmol CO_2 m^{-2} s^{-1} (t-test; df=159, P=0.7%), but there are only 11 hours of data (6% of the total) from this direction. A lower biotic flux in the westerly directions

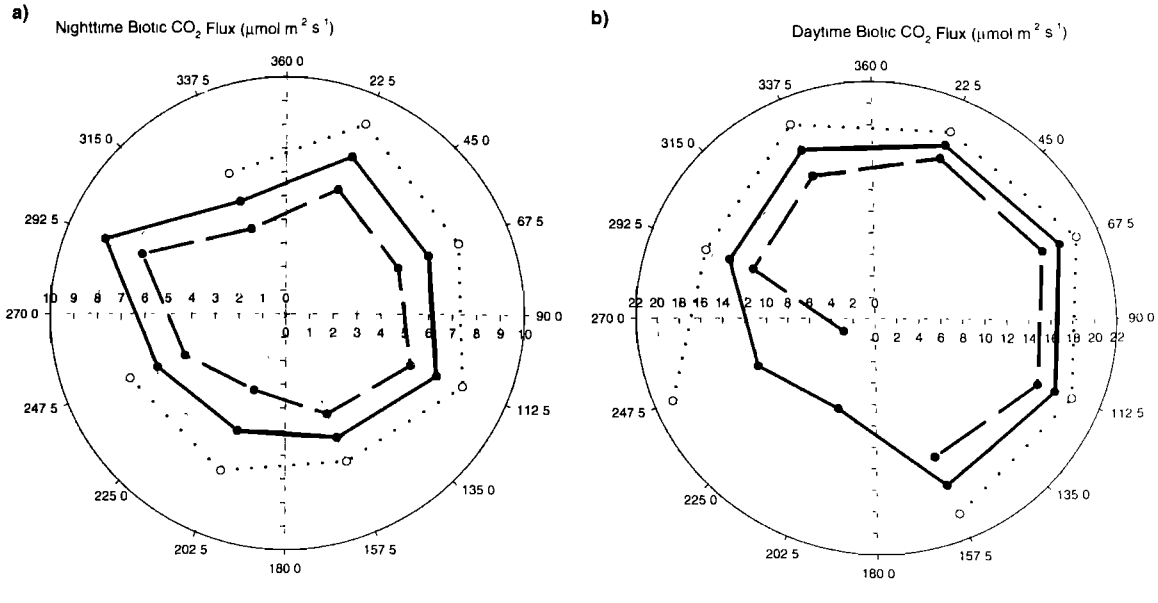

Figure A4. Variation of the biotic flux with wind direction for the period October 16 to December 10, 1995 for (a) daytime at high insolation (> 500 W m^{-2}) and (b) nighttime (1800 to 0500).

may be due to the presence of the tower or the disturbed area around the access trails. In any case, given the preponderance of easterly winds, this will have only a small impact on the overall data set.

A3.3. Turbulence statistics. The variation of turbulence and mean flow statistics with stability and wind direction was also examined. The details of the analysis will be presented in a companion paper (Y. Malhi et al., manuscript in preparation 1998), but a few relevant results are described here. The ratio σ_w/u_* is expected to be constant in an idealized surface layer in near-neutral conditions [*Panofsky and Dutton*, 1984], and departure from this constancy can be an indicator of wake turbulence. For the current data set, the ratio was a well-behaved function of stability for $|(z-d)/L| < 2$, and the near-neutral value was 1.37±0.27 (1 standard deviation, n=4782), slightly higher than the *Panofsky and Dutton* [1984] value of 1.25. As a function of wind direction, the mean varies between 1.25 and 1.60, but there is no obvious correlation with the position of the tower or the anemometer struts.

A3.4. Flow distortion by the tower. The vertical angle of the mean flow relative to the anemometer θ can be an indicator of flow distortion effects. The general variation of θ with wind direction is consistent with the anemometer being inclined at 2° to the mean flow plane, a factor that is automatically compensated for in the coordinate rotation algorithms. When the wind is from a westerly direction, however, there is an enhanced flow angle of 2° (night) to 6° (high heat flux noon conditions), suggesting the presence of flow distortion partially induced by solar heating of the tower. However, a detailed analysis (to be presented in a forthcoming paper) suggests that such small distortions do not have a significant impact on the measured flux.

A3.5. Conclusions on wind direction analysis. The above wind direction analysis has shown that there is little evidence of significant spatial variability north, east, and south of the tower. Within the constraints imposed by the noisiness of the data, this implies that there are no small-scale local events, such as tree fall and canopy gaps [*Keller et al.*, 1996], that are having a disproportionate impact on the measured fluxes. There is more evidence of a different regime to the west of the instrument, which may be due the disturbance around the access trail and/or to the presence of the tower itself. The tendency in this direction is to less uptake in the day and slightly more respiration at night (although the statistical confidence is not very high), implying that any tower/trail disturbance may bias the data set to a net source of CO_2. However, in the analyses in this paper, data from this direction have not been filtered out, as their impact on the overall results is negligible.

A4. Influence of Rain

The instrumentation is designed to accurately measure CO_2 fluxes in all conditions, including rainfall rates up to 300 mm hr^{-1}. The effect of rain on measurements can be assessed by comparing the light response curves in rain and nonrain conditions, as shown in Figure A5. The above-canopy flux is used rather than the biotic flux because it is a more extensive data set. For most of the data points, the light-response curve is very similar in rainy and nonrainy conditions, with the slightly more positive values in rain being due to the fact that the rain data are biased toward windy conditions with little within-canopy storage (in fact, the above-canopy flux in rainy conditions tends toward the biotic flux). There are a few events with large positive fluxes, which may be due to the flushing of CO_2 from the soil pores at the onset of rain. If rain does introduce any measurement error, it is to bias the data toward more positive fluxes (i.e., less carbon uptake).

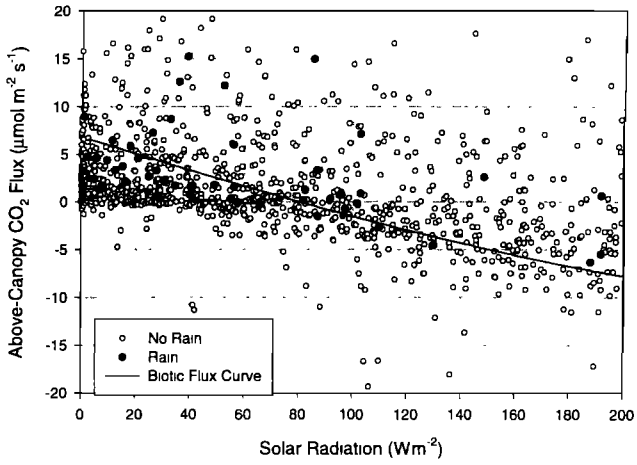

Figure A5. Light-response curves of the above-canopy flux in rain (solid circles) and nonrain conditions over the entire year (open circles). The line represents the light-response curve of the biotic flux (see *Figure 6a*).

A5. Fitting an Empirical Model

A variety of nonlinear curve fits were compared with the data. The aim of these fits was to capture the mean behavior of the forest with as simple an equation as possible, allowing interpolation to fill in gaps in the data, rather than representing physiological processes in detail.

The net CO_2 flux was separated into photosynthesis and respiration components, such that

$$F = R(T) - A(S)$$

where F is net ecosystem CO_2 exchange (µmol m^{-2} s^{-1}), $R(T)$ is dark respiration rate of soil and vegetation (µmol m^{-2} s^{-1}), T is soil temperature at 5 cm depth, $A(S)$ is photosynthetic rate (µmol m^{-2} s^{-1}), and S is incoming solar radiation (W m^{-2}).

The ecosystem respiration was modeled as an exponential function of the measured soil temperature. *Meir et al.* [1996] estimated that soil respiration accounted for approximately 84% of the ecosystem respiration at Reserva Jaru, Rondonia, and determined a Q_{10} of 2.3 for an exponential fit to the data. Incorporating this Q_{10} value into the nocturnal respiration measured in Manaus,

$$R = \langle R \rangle e^{\alpha(T-\langle T \rangle)} \quad \text{(A1)}$$

where $\langle R \rangle$ is the mean measured nocturnal respiration (6.46 µmol m^{-2} s^{-1}, $\langle T \rangle$ is the mean measured nocturnal soil temperature (24.3°C), and $\alpha = (\ln Q_{10})/10$. This linear-averaging approximation is valid as long as $|T-[T]| << 10/\ln Q_{10}$.

Leaf dark respiration rates are here assumed to behave similarly to soil respiration, whereas, in fact, they may decrease significantly during the day [e.g., *Villar et al.*, 1994]. Other modeling studies [*Williams et al.*, 1998] deal more explicitly with these terms. The photosynthesis term was derived from the data as follows.

A5.1. Light response only. An adequate fit to the data is obtained by a third-order polynomial of the form

$$A = a_1 S + a_2 S^2 + a_3 S^3$$

with the optimal values of the parameters being $a_1 = k = -0.097$ μmol J^{-1} (quantum yield × 2.16), $a_2 = 1.355 \times 10^{-4}$ μmol m^{-2} $s^{-1}/(W\ m^{-2})^2$, and $a_3 = -6.333 \times 10^{-8}$ μmol m^{-2} $s^{-1}/(W\ m^{-2})^3$ (r^2 =0.69).

There was no significant increase in quality of the fit when higher-order polynomials were used. This polynomial provides an adequate fit to the data, but the parameters a_2 and a_3 have no direct biological interpretation. A more physiologically interpretable equation is a nonrectangular hyperbola (see Figure 7a), with A being a solution of

$$M.A^2 - (kS + A_{max})A + kSA_{max} = 0 \quad \text{(A2)}$$

where A_{max} = maximum photosynthetic rate (μmol m^{-2} s^{-1}), k = initial slope of photosynthetic curve (quantum yield × 2.16), and M = the convexity of the hyperbola ($0 < M < 1$). The optimal values of the parameters are $M = 0.80$, $k = -0.092$ μmol J^{-1}, and $A_{max} = -26$ μmol m^{-2} s^{-1} (r^2=0.68).

A5.2. Including a VPD response. Introduction of a simple VPD response resulted in a significant improvement in quality of fit. Various VPD-response functions were tried, and a simple linear multiplying factor was found to be adequate (Figure 6b)

$$A = f(S)(1-wD) \quad \text{(A3)}$$

where D is the water vapor deficit (kilopascals) and w is a multiplying factor (kPa^{-1}). Using a nonrectangular hyperbola (see Figure 6), the values that gave an optimum fit were $M = 0.62$, k = -0.104 μmol J^{-1}, $A_{max} = -44$ μmol m^{-2} s^{-1}, and $w = 0.2044$ kPa^{-1}. The r^2 value increased to 0.74 (that is, an additional 6% of the total variance of the data is explained). As this forest does not light saturate within normal light levels, the value of A_{max} does not have any direct biological interpretation.

A5.3. Including seasonal variation in photosynthesis. The analysis presented above demonstrated that a simple, calibrated hourly light and VPD response model is sufficient to describe the CO_2 fluxes at any particular time of the year, but to consider the year as a whole, we introduce seasonality in photosynthesis as an additional variable factor. As the mechanism for this observed seasonality is not currently understood, a simple empirical fit to the observations will suffice for present purposes.

Thus, in a revised empirical fit model, the carbon fluxes are described by a light and VPD response, as in (A2) and (A3), but the maximum photosynthesis G_{max} is allowed to vary as a function of time of year. A third-order polynomial was found to be an adequate descriptor of the variation of G_{max}. The model was fitted to the entire CO_2 flux data set using a least squares iteration. However, a point of difficulty arises because the model best describes the biotic flux, whereas for much of the year, the only carbon flux data collected were above-canopy fluxes. This difficulty can be ameliorated by fitting the accumulated model predictions to the accumulated flux measurements, as on a 24-hour basis, the storage term sums to zero and thus the accumulated above-canopy flux is approximately equal to the accumulated biotic flux. Nonexact matching on a day-to-day basis will be much less significant when fitting the year as a whole. The best fit to the data was the third-order polynomial $G_{max} = (b_0 + b_1 d + b_2 d^2 + b_3 d^3)$ μmol m^{-2} s^{-1}, where $b_0 = -25.05$, b_1 = -0.18839, $b_2 = 9.824 \times 10^{-4}$, $b_3 = -1.486 \times 10^{-6}$, and d = day since September 1, 1995). As mentioned above, the magnitude of G_{max} does not have direct biological significance, as the forest does not light saturate at high insolation.

Acknowledgements. We thank Jon Lloyd, Patrick Meir, Ari Marques Filho, João Matos, John Moncrieff, Paul Jarvis, John MacIntyre, Jon Massheder, Martin Hodnett, Carlos Nobre, and John Gash for technical and logistical support, and Afonso for invaluable help in the field. This work was made possible via a grant from the U.K. Natural Environmental Research Council (NERC) Terrestrial Initiative in Global and Environmental Research (TIGER) program. The work forms part of the Anglo-Brazilian Climate Observation Study (ABRACOS), supported by the U.K. Overseas Development Administration (ODA) in collaboration with the Agência Brasileira de Cooperação (ABC). We gratefully acknowledge the help of Instituto Nacional de Pesquisas Espaciais (INPE) and Empresa Brasileira de Pesquisa Agropecuaria (EMBRAPA) in providing logistical support for the project.

References

Baldocchi, D., R. Valentini, S. Running, W Oechel, and R Dahlman, Strategies for measuring and modelling carbon dioxide and water vapour fluxes over terrestrial ecosystems, *Global Change Biol.*, *2*, 159-168, 1996.

Chauvel, A , M. Grimaldi, and D. Tessier, Changes in soil pore-space distribution following deforestation and revegetation: An example from the Central Amazon Basin, Brazil, *For. Ecol. Manage*, *38*, 259-271, 1991.

Correa, J. C.. Características físico hídricas dos solos latosollo amarelo, podzolico vermelho amarelo e podzol hidromórfico do estado do Amazonas, *Pesquis. Agropecuaria Bras.*, *20*, 1317-1322, 1984.

Culf, A. D., G. Fisch, and M. G. Hodnett, The albedo of Amazonian forest and ranch land, *J. Clim.*, *8*, 1544-1554, 1995.

Fan, S. -M., S. Wofsy, P. Bakwin, and D. Jacob, Atmospheric-biosphere exchange of CO_2 and O_3 in the central Amazon forest, *J. Geophys. Res.*, *95*, 16,851-16,864, 1990.

Farquhar, G. D., S. von Caemmerer, J. A Berry, A biochemical model of photosynthetic CO_2 assimilation in leaves of C_3 species, *Planta*, *149*, 79-90, 1980.

Food and Agriculture Organization, Forest Resources Assessment 1990 – Tropical Countries, *For Pap.*, *112*, Rome, 1993

Franken, M , U. Irmler, and H Klinge, Litterfall in inundation, riverine and terra firme forests of Central Amazonia. *Trop. Ecol* , *20*, 225-235, 1979.

Goulden, M. L., J. W Munger, S. -M. Fan, B. C. Daube, and S C. Wofsy, Measurements of carbon sequestration by long-term eddy covariance: Methods and a critical evaluation of accuracy, *Global Change Biol* , *2*, 169-182, 1996

Grace, J., J. Lloyd, J. McIntyre, A. C. Miranda, P. Meir, H. Miranda, J M Moncrieff, J Massheder, I. R. Wright, and J. Gash, Fluxes of carbon dioxide and water vapour over an undisturbed tropical rainforest in south-west Amazonia, *Global Change Biol.*, *1*, 1-12, 1995a.

Grace, J., et al , Carbon dioxide uptake by an undisturbed tropical rain forest in South-West Amazonia 1992-1993, *Science*, *270*, 778-780, 1995b.

Grace, J., Y. Malhi, J. Lloyd, J. McIntyre, A. C. Miranda, P. Meir. And H. S. Miranda, The use of eddy covariance to infer the net carbon dioxide uptake of Brazilian rain forest, *Global Change Biol.*, *2*, 209-218, 1996.

Grace, J., Y. Malhi, N. Higuchi, and P. Meir, Carbon fluxes and productivity of tropical forests, in *Terrestrial Global Productivity: past, present and future*, edited by H.A. Mooney, J. Roy and B. Saugier, Academic Press, San Diego, in press, 1999.

Hodnett, M. G., S. P. da Silva, H. R. da Rocha, and R C. Senna, Seasonal soil water storage changes beneath central Amazonian rainforest and pasture, *J. Hydrol. 170*, 233-254, 1995.

Hodnett, M. G , J. Tomasella, A. O. Marques Filho, and M. D. Oyama, Deep water uptake by forest and pasture in central Amazonia: Predictions from long-term daily rainfall data using a simple water balance model, in *Amazonian Deforestation and Climate*, edited by J. H. C. Gash et al., pp. 79-99, John Wiley, New York, 1996.

Jarvis, P. G., and J. W Leverenz, Productivity of temperate, deciduous and evergreen forests, in *Physiological Plant Ecology IV, Ecosystems Processes· Mineral Cycling, Productivity and Man's Influence*, edited by O.L. Lange et al., pp. 233-261, Springer-Verlag, Berlin, 1983.

Jordan, C. F., Productivity of tropical rain forest ecosystems and the implications for their use as future wood and energy sources, in

Tropical Rain Forest Ecosystems: Structure and Function, edited by F. B. Golley, pp. 117-136, Elsevier, New York, 1983.

Kaimal, J. C., J. C. Wyngaard, Y. Izumi, and O. R. Cote, Spectral characteristics of surface-layer turbulence, *Q. J. R. Meteorol. Soc.*, *98*, 563-589, 1972.

Katul, G. G., C. R. Chu, J. D. Albertson, and M. B. Parlange, The low-wavenumber spectral characteristics of velocity and temperature in the atmospheric surface layer, *J. Geophys. Res.*, *100*, 14,243-14,255, 1995.

Keller, M., D. A. Clark, D. B. Clark, A. M Weitz, and E. Veldkamp, If a tree falls in the forest..., *Science*, *273*, 5272, 1996.

Klinge, H., W. A Rodrigues, E. Brunig, and E. J. Fittkau, Biomass and structure in a central Amazonian rainforest, in *Tropical Ecological Systems. Trends in Terrestrial and Aquatic Research*, edited by F. B. Golley and E. Medina, pp. 115-122, Springer-Verlag, New York, 1975.

Lee, X., On micrometeorological observations of surface-air exchange over tall vegetation, *Agric. For. Meteorol.*, 2545, pp. 1-11, 1998.

Lloyd, C. R., The effect of heterogeneous terrain on micromet flux measurements· A case study from HAPEX-Sahel, *Agric. For. Meteorol.*, 73, pp. 209-216, 1995.

Lloyd, J., J. Grace, A. C. Miranda, P. Meir, S. C. Wong, H. Miranda, I. Wright, J. H. C. Gash, and J. McIntyre, A simple calibrated model of Amazon rainforest productivity based on leaf biochemical properties, *Plant Cell Environ.*, *18*, 1129-1145, 1995.

Luizão, F. J., and H. O. R. Schubert, Litter production and mineral element input to the forest floor in a Central Amazonian forest, *Geojournal*, *19*, 407-417, 1989.

Luizão, F. J., Ecological studies in contrasting forest types in Central Amazonia, Ph.D. thesis, University of Stirling, Stirling, Scotland, 1995.

McWilliam, A. -L. C., J. M. Roberts, O. M. R. Cabral, M. V. B. R. Leitao, A. C. L. de Costa, G. T. Maitelli, and C. A. G. P. Zamparoni, Leaf area index and above-ground biomass of *terra firme* rain forest and adjacent clearings in Amazonia, *Functional Ecol.*, *7*, 310-317. 1993.

Meir, P., The exchange of carbon dioxide in tropical forest, Ph.D. Thesis, Uni. of Edinburgh, Edinburgh, Scotland, 1996.

Meir, P., J. Grace, A. C. Miranda, and J. Lloyd, Soil respiration measurements in the Brazil forest and cerrado vegetation during the wet season, in *Amazonian Deforestation and Climate*, edited by J. H. C. Gash et al., pp. 319-330, John Wiley, New York, 1996.

Mello Ivo, W., S. Ferreira, Y. Biot, and S. Ross, Nutrients in soil solution following selective logging of a humid tropical '*terra firme*' forest north of Manaus, Brazil, *Environ. Geochem. Health*, *18*, 69-75, 1996.

Moncrieff, J. B., Y. Malhi, and R. Leuning, The propagation of errors in long-term measurements of land-atmosphere fluxes of carbon and water, *Global Change Biology*, *2*, 231-240, 1996.

Moncrieff , J. B., J. M. Massheder, H. De Bruin, J. Elbers, T. Friborg, B. Huesunkveld, P. Kabat, S. Scott, H. Soedaard, and A. Verhoef, A system to measure surface fluxes of momentum, sensible heat, water vapor and carbon dioxide, *J. Hydrology*, *188/189*, 589-611, 1997.

Moore, C. J., Frequency response corrections for eddy correlation systems, *Boundary Layer Meteorol.*, *37*, 17-35, 1986

Müller, M. H., and J. Nielsen, Production brutes pertes par respiration et production nette dans la foret ombrophile tropicale, *Foresel Forsogsaves Dan.*, *29*, 69-160, 1965.

Nepstad, D. C , C. R. de Carvalho, E. A. Davidson, P. H. Jipp, P. A. Lefebvre, G. H Negreiros, E. D. da Silva, T. A. Stone, S. E. Trumbore, and S. Vieira, The role of deep roots in the hydrological and carbon cycles of Amazonian forests and pastures, *Nature*, *372*, 666-669, 1994

Oikawa, T., Simulation of forest carbon dynamics based on a dry matter production model, 1, Fundamental model structure of a tropical rainforest ecosystem, *Bot. Mag., Tokyo*, *98*, 225-238, 1985.

Panofsky, H. A. and J. A. Dutton, *Atmosphere Turbulence – Models and Methods for Engineering Applications*, John Wiley and Sons, New York, 1984

Phillips, O. L. et al., Changes in the carbon balance of tropical forests: evidence from long-term forest plots, *Science*, in press, 1998.

Rannik, U., T. Vesala, and R. Kesinken, On the damping of temperature fluctuations in a circular tube relevant to the eddy covariance measurement technique, *J. Geophys. Res.*, *102*, 12,789-12,794, 1997.

Raupach, M. R., J. J. Finnigan, and Y. Brunet, Coherent eddies and turbulence in vegetation canopies: The mixing-layer analogy, *Boundary Layer Meteorol.*, *78*, 351-382, 1996

Ribeiro, M. N. G., and J. Adis, Local rainfall variability – A potential bias for bioecological studies in the central Amazon, *Acta Amazonica*, *14*, 159-174, 1984.

Ruimy, A., P. G. Jarvis, D. D. Baldocchi, and B. Saugier, CO_2 fluxes over plant canopies and solar radiation: A review, *Adv. Ecol. Res.*, *26*, 1-81. 1995.

Sanchez, P. A., Soils, in *Tropical Rain Forest Ecosystems: Biogeographical and Ecological Studies*, edited by H. Lieth and M.J A. Werger, pp. 132-161, Elsevier, New York, 1989.

Schimel, D. S., Terrestrial ecosystems and the global carbon cycle, *Global Change Biol.*, *1*, 77-91, 1995.

Schuepp, P. H., M. Y. Leclerc, J. I. Macpherson, and R. L. Desjardins, Footprint prediction of scalar fluxes from analytical solutions of the diffusion equation, *Boundary Layer Meteorol.*, *50*, 355-373, 1990.

Shuttleworth, W. J., Micrometeorolgy of temperate and tropical forest, *Philos. Trans. R. Soc. London, Ser. B*, *324*, 299-334, 1989.

Shuttleworth, W. J., et al., Eddy correlation measurements of energy partitioning for Amazon forest, *Q. J. R. Meteorol. Soc.*, *110*, 1143-1162, 1984.

Taylor, J. A., and J. Lloyd, Sources and sinks of atmospheric CO_2, *Aust. J. Bot.*, *40*, 407-418, 1992

Villar, R., A. A. Held, and J. Merino, Comparison of methods to estimate dark respiration in the light in leaves of two woody species, *Plant Physiol.*, *105*, 167-172, 1994.

Webb, E. K., G. I. Pearman, and R. Leuning, Correction of flux measurements for density effects due to heat and water vapour transfer, *Q. J. R. Meteorol. Soc.*, *106*, 85-100, 1980.

Weiss, A. and J. M. Norman, Partitioning solar radiation into direct and diffuse, visible and near-infrared components, *Agric. For. Meteorol.*, 34, 205-313, 1985.

Whittaker, R. H., and G. E. Likens, The biosphere and man, in *Primary Productivity of the Biosphere*, edited by R. H. Whittaker and G. E. Likens, pp. 305-328, Springer-Verlog, New York, 1975.

Williams, M., Y. Malhi, A. D. Nobre, E. B. Rastetter, J. Grace, and M. G. P. Pereira, Seasonal variation in net carbon exchange and evapotranspiration in a Brazilian rain forest: A modelling analysis, *Plant Cell Environ.*, in press, 1998.

A. Culf, Institute of Hydrology, Wallingford, England, United Kingdom.

J. Grace, B. Kruijt, Y. Malhi (corresponding author), and S. Scott Institute of Ecology an Resource Management, The University of Edinburgh, Darwin Building, Mayfield Road, Edinburgh EH9 3JU, Scotland, United Kingdom. (YMalhi@ed.ac.uk)

A. D. Nobre and M. G. P. Pereira, Instituto Nacional de Pesquisas da Amazonia, Manaus, Brazil.

(Received September 23, 1997; revised August 5, 1998;
accepted August 12, 1998.)